File with N74-35182

NASA CR - 132512

ATS-51022

STUDY TO IMPROVE THE LOW FREQUENCY NOISE CHARACTERISTICS OF (Hg,Cd)Te DETECTORS

HONEYWELL
Radiation Center
2 Forbes Road
Lexington, Massachusetts 02173

NASA CR-132512

STUDY TO IMPROVE THE LOW FREQUENCY NOISE CHARACTERISTICS OF (Hg,CD)Te DETECTORS

By Robert M. Broudy

Prepared under Contract No. NAS1-10682 by
HONEYWELL RADIATION CENTER
2 Forbes Road
Lexington, Massachusetts 02173

for

NATIONAL AERONAUTICS AND SPACE ADMINISTRATION

TABLE OF CONTENTS

SECTION	TITLE	PAGE
1	INTRODUCTION	1-1
1.1	SUMMARY	1-1
1.2	RESULTS AND CONCLUSIONS	1-1
1.3	HISTORY	1-2
1.4	DIRECTIONS FOR FUTURE WORK	1-3
2	ACKNOWLEDGEMENTS	2-1
3	CLASSICAL THEORY OF 1/f NOISE	3-1
3.1	GENERAL PARAMETERS DESCRIBING 1/f NOISE	3-1
3.2	CLASSICAL THEORY FUNDAMENTALS	3-3
3.3	McWHORTER'S SURFACE MODEL	3-5
3.4	HOOGE'S BULK MODEL FOR 1/f NOISE	3-7
4	EARLY EXPERIMENTAL CORRELATIONS	4-1
5	NEW APPROACHES	5-1
6	NEW PHENOMENOLOGICAL THEORY	6-1
7	SPECIAL EXPERIMENTAL TECHNIQUES-SURFACES & VOLUMES	7-1
7.1	PARALLEL PLATE CONFIGURATION	7-2
7.2	DOT CONFIGURATION	7-3
8	MEASUREMENT METHODS	8-1
8.2	DETECTOR BIAS	8-1
8.3	AMPLIFIER	8-2
8.4	MEASURING APPARATUS	8-2
9	LOW FREQUENCY ANOMALIES	9-1
9.1	CONTACT EFFECTS - 1/f NOISE FROM CONTACTS	9-1
9.2	OTHER SPURIOUS EFFECTS	9-2

TABLE OF CONTENTS (Continued)

SECTION	TITLE	PAGE
10	NOISE FROM DOTS--ORIGIN OF 1/f NOISE	10-1
10.1	EXPERIMENTAL	10-1
10.2	DIMENSIONAL ANALYSIS	10-4
10.3	SIGNIFICANCE OF RESULTS-ORIGIN OF 1/f NOISE	10-5
11	INITIAL APPLICATION OF TECHNIQUE	11-1
11.1	GENERAL APPROACH	11-1
11.2	DIRECTIONS FROM PARALLEL PLATE RESULTS	11-1
12	FIELD DEPENDENT EFFECTS- 1/f NOISE AND SWEEPOUT IN DETECTORS	12-1

SECTION 1

INTRODUCTION

1.1 SUMMARY

This is the final report on NASA Contract NAS1-10682, entitled "Study to Improve the Low Frequency Noise Characteristics of (Hg, Cd)Te Detectors." Work on the contract was performed during the period from April 16, 1971 through August 31, 1973.

The broad objectives of this program have been to identify the sources of 1/f noise in 15-micron n-type (Hg,Cd)Te detectors operating at 77°K, and to initiate methods for reducing this noise. These objectives have been achieved.

The investigations included: evaluation of the influence of material properties and detector processing techniques; determination of the relative importance of surfaces, volume regions, and contacts; and generation of theoretical models for guidance of the experimental work.

1.2 RESULTS AND CONCLUSIONS

The significant results of this program include three major accomplishments:

- EXPERIMENTAL TECHNIQUES

  The means were provided for simple, direct, evaluation of the influence of surface preparation and properties on 1/f noise, by the development of special experimental techniques. These techniques enabled the separation of surface from volume and provided unique information on the nature of 1/f noise mechanisms.

- ORIGIN OF 1/f NOISE

  It was demonstrated that 1/f noise in (Hg,Cd)Te detectors (and possibly in other systems) is directly related to gr noise, and that the component of gr noise due to surface recombination generally leads to more 1/f noise. Strong circumstantial evidence was obtained that 1/f noise is in fact due to macroscopic fluctuations in current which are initiated by microscopic irregularities.

- REDUCTION OF 1/f NOISE

  Recommendations were developed and work was initiated for processing methods to reduce 1/f noise in (Hg,Cd)Te detectors, based on the experimental and analytical methods developed during this program.

1.3 HISTORY

The program essentially developed into four phases. The initial phase includes work performed from April 16, 1971 through September 31, 1971. During this period, the program was initiated, material parameters describing 1/f noise were determined in terms of existing theory and related to experimental results, and electrical and photoconductive evaluations were performed on a specially grown ingot. This phase showed that 1/f noise in (Hg, Cd)Te detectors behaves similarly to that in other devices, with equally limited agreement with experiment. The importance of uniform material properties was demonstrated.

The second phase covers the period from October 1, 1971 through December 31, 1971, during which the contract was extended at no cost, and existing 1/f noise data at the Radiation Center were reviewed and compared with material properties in light of the results from the first phase. This review indicated the direction for further work.

The third phase covers the period from January 1, 1972 through May 31, 1972. During Phase III a thorough re-evaluation of the program was performed in light of several recent significant developments concerning 1/f noise which Honeywell felt would directly influence the remainder of the program. These developments included: (a) an improved quantitative understanding of electrical properties of (Hg,Cd)Te material, (b) new theoretical advances in 1/f noise, (c) the results of recent field effect measurements reported in the literature (mostly on silicon), and (d) the existence of low frequency noise data which had become available from routine evaluation measurements recently introduced at the Radiation Center. On the basis of work during Phase III, Honeywell formulated a plan for the remainder of the program, Phase IV.

Phase IV covers the period from June 1, 1972 to the end of the program. Limitations of previous theories of 1/f noise were recognized and the approach to analysis of results was changed in the direction of new theoretical advances, which consider that

1/f noise originates in macroscopic current fluctuations. It seemed clear that 1/f noise is neither a volume-only nor a surface-only phenomenon, and that it must originate in a complex volume-surface interaction. It was decided early that this interaction probably involves surface space charge regions, i.e., depletion and accumulation layers. Subsequent experimental and theoretical results, summarized below, substantiated this viewpoint and led to recommendations and initiation of processing methods for reduction of 1/f noise in detectors.

1.4 DIRECTIONS FOR FUTURE WORK

The results of the program indicate two parallel not necessarily independent, directions for investigation. First, it is clear that the technique and concepts developed here are ripe for exploitation to determine processing methods for reduction of 1/f noise in (Hg,Cd)Te photoconductive detectors over the full wavelength region. Moreover, they can also be applied to a wide range of other materials and types of devices. Secondly, directions have been indicated for more detailed analysis of mechanisims of 1/f noise in general, with the hope of finally achieving a complete fundamental comprehension of this fascinating phenomenon.

SECTION 2

ACKNOWLEDGEMENTS

This work was initiated by Dr. Marion B. Reine, who was the Project Engineer during the earlier phases of the program and wrote most of the sections pertaining thereto. It is a pleasure to acknowledge his continuing suggestions and assistance throughout the program. He provided the excellent foundation that set the way for the work that followed.

I am happy also to acknowledge the invaluable contributions of Mr. Gregory P. Lafyatis, who developed the instrumentation and equipment, and obtained the experimental data during the latter phase of the program. His suggestions and insights on both methods and theory were both helpful and stimulating.

SECTION 3

CLASSICAL THEORY OF 1/f NOISE

3.1 GENERAL PARAMETERS DESCRIBING 1/f NOISE

In general, for any model, 1/f noise is included in the total detector noise, v_n, in the following form:

$$v_n^2 = v_j^2 + v_{gr}^2 + v_{1/f}^2 \tag{3.1}$$

$$v_{1/f}^2 = K/f \tag{3.2}$$

where v_j is the Johnson noise, v_{gr}, the generation-recombination (gr) noise, and the 1/f noise squared, $v_{1/f}^2$, has the form of a constant times the inverse linear power of the frequency. All material and physical phenomena are included in the constant K (except for the inverse frequency dependence itself, of course). Subsequent discussion will neglect the Johnson noise, which is usually small for practical detector operation. It is important to note that generally K varies as the square of the current.

A parameter which is more important than the strength of the 1/f noise is the frequency at which the 1/f noise voltage equals the generation-recombination plateau noise voltage. This frequency will be referred to as the 1/f noise corner frequency and denoted by f_c.

The corner frequency f_c can be expressed as:

$$f_c = (K/v_{gr})^2 \tag{3.3}$$

where K is defined by equation 3.2, and where v_{gr} is the frequency-independent generation-recombination noise voltage. Over the frequency range for which the g-r noise is independent of frequency, the detectivity (neglecting Johnson noise) can be expressed as:

$$D^*_\lambda = \frac{R_\lambda \left[A_D\right]^{1/2}}{v_{gr}} (1 + f_c/f)^{-1/2} \tag{3.4}$$

where R_λ is the responsivity and A_D is the detector active area.

PCF
CLASSIFICATION (If Any)

An experimental determination of f_c can be obtained from detectivity (or noise) values at two frequencies; f_ℓ for the lower frequency and f_h for the higher frequency. Let α denote the ratio

$$\alpha = \frac{D^*(f_h)}{D^*(f_\ell)} = \frac{v_n(f_\ell)}{v_n(f_h)} \tag{3.5}$$

then

$$f_c = f_\ell(\alpha^2-1)/(1-\alpha^2/f_h) \tag{3.6}$$

The corner frequency f_c is a very useful parameter. Unlike the 1/f coefficient C_1, it is directly measurable. Furthermore, it specifies directly the useful range of a detector. An explicit expression for f_c can be derived by using the following expression for the generation-recombination noise voltage in a near-intrinsic semiconductor:[1,2]

$$v_{gr} = \frac{2E}{n_o} (\ell/w)^{1/2} (\tau/d) (\eta Q_B + \eta_\ell Q_\ell)^{1/2} (\Delta f)^{1/2} \tag{3.7}$$

where n_o is the free electron concentration, τ is the photoconductive response time, η is the optical quantum efficiency, Q_B is the incident background photon flux, and η_ℓ and Q_ℓ are analogous terms referring to lattice-induced electron-hole pair generation.

The effect of detector temperature and background can be explicitly evaluated from material parameters by noting that $\eta\ Q_B$ represents the creation of electron-hole pair by the steady state background photon flux, and $\eta_\ell\ Q_\ell$ represents the creation of electron-hole pairs by equilibrium thermal exictation. That is, both thermally and optically generated carriers are equivalent noise sources. In fact, Schlickman[1] has shown that the following condition of dynamic equilibrium holds:

$$\eta\ Q_B + \eta_\ell\ Q_\ell = \left(\frac{np}{n+p}\right) d/\tau \tag{3.8}$$

The carrier concentrations are given by:

$$\begin{aligned} n &= n_o + n_b \\ p &= p_o + p_b \end{aligned} \tag{3.9}$$

where $n_b (=p_b)$ is the concentration of excess electron-hole pairs due to background radiation above the thermal equilibrium concentrations, n_o and p_o. For n-type intrinsic photoconductors, such as (Hg,Cd)Te, one finds $n_o \gg n_b$, then the creation expression, equation 3.8, becomes:

$$\eta Q_B + \eta_\ell Q_\ell \tilde{=} (p_b + p_o)\ (d/\tau) \tag{3.10}$$

Then equation 3.7 can be written:

$$v_{gr} = \frac{2E}{n_o} \left(\frac{\ell}{wd}\right)^{1/2} \tau^{1/2} \left[p_B + p_o\right]^{1/2} \Delta f^{1/2} \tag{3.11}$$

In this expression, the contributions of optically and thermally generated carriers appear directly and independently in the terms p_B and p_o. Thus, for a given model of 1/f noise (which determines the parameter K) f_c can be determined from 3.3 and 3.11.

3.2 CLASSICAL THEORY FUNDAMENTALS

From fairly general noise theory arguments[3,4] the 1/f noise voltage $v_{1/f}$ in (Hg,Cd)Te detectors can be written as:

$$v_{1/f}^2 = \frac{C_1}{d} \frac{\ell}{w} E^2 \frac{\Delta f}{f} \tag{3.12}$$

where ℓ, w and d are the length, width, and thickness of the detector, E is the dc bias electric field, Δf is the noise bandwidth, f is the frequency, and C_1 is a coefficient which gives the strength of the 1/f noise. In particular, C_1 should be independent of the detector dimensions.

It is important to note that the derivation of equation 3.12 and similar equations is based on what we call "classical theory" assumptions, which underlie the majority of noise theory[5,6]. Specifically, it is assumed that the noise in question originates from microscopic localized noise generators distributed at appropriate regions for each model. Thus, all dimensional relations depend on this assumption. It is interesting that very little, if any, experimental verification has been reported of the predicted dimensional behavior for 1/f noise, whereas thorough substantiation has been obtained for other sources, such as Johnson and g-r noise.

PCF
CLASSIFICATION (If Any)
DO NOT TYPE OR STAMP

In this "classical" approach, f_c can be determined by combining equations 3.3, 3.7 and 3.12 to give the following expression for the corner frequency f_c:

$$f_c = \frac{C_1 \, n_o^{\,2} \, d}{4 \, \tau^2 \, (\eta \, Q_B + \eta_\ell \, Q_\ell)} \tag{3.13}$$

This equation illustrates, for example, that f_c depends on the detector thickness but not on the active area dimensions. It also shows the strong dependence of the corner frequency on carrier concentration and on response time.

The corner frequency can be expressed as well in terms of p_B and p_o by using equations 3.11 and 3.13.

$$f_c = C_1 \, n_o^{\,2} / 4 \, \tau (p_B + p_o) \tag{3.14}$$

When the detector temperature is sufficiently low that thermally generated carriers become negligible compared to optically generated carriers, then $\eta_\ell \, Q_\ell \ll \eta \, Q_B$, $p_o \ll p_B$, and the detector becomes background limited ("BLIP"). The proper expression for v_{gr} is then obtained by setting $\eta_\ell \, Q_\ell = 0$. Then f_c is found either by placing equation 3.7 into equation 3.3 or by noting that p_B is $\eta\tau \, Q/d$ in equation 3.14:

$$f_c^{\,BLIP} = \frac{C_1 \, n_o^{\,2} \, d}{4 \, \tau^2 \, \eta \, Q_B} \tag{3.15}$$

On the other hand, when elevated detector temperature raises p_o above p_B, then one should use equation 3.13 and 3.14 with p_B set = 0, and f_c becomes

$$f_c^{\,+} = \frac{C_1 \, n_o^{\,2}}{4 \, \tau \, p_o} \tag{3.16}$$

The "+" superscript is used in analogy with similar terminology for D*, which is often designated as D^+, when v_{gr} is determined by thermal generation. Thus D^*_λ is determined from 3.4 and 3.11 and 3.12 with $p_o = 0$, and D^+_λ can be found from 3.4 and 3.14, with p_o being determined from semiconductor equilibrium conditions.

PCF

CLASSIFICATION (If Any)

The effect of detector temperature is shown in Figure 3.1, which presents the result of calculations of D^+_λ and D* for (Hg,Cd)Te, using experimental time constants as a function of detector temperatures for a ctuoff wavelength of 13 microns. Note that D* remains independent of temperature until the detector temperature increases above the D* - D^+ crossover. Then, detectivity decreases along the D^+ curve as temperature rises further. The effect depends on background as shown. D^+_{rad} represents the best possible D*, since it has been calculated by assuming radiative lifetime.

Equations 3.15 and 3.16 provide expressions to be used for specific models based on the classical theory. For purposes of completeness and historical exposition, two such models are discussed below:

3.3 McWHORTER'S SURFACE MODEL

McWhorter developed a model for 1/f noise in semiconductors based on the existence of surface traps. Fluctuations in the capture and release of bulk electrons at these surface traps produce fluctuations in the bulk electron concentration and consequently in the conductivity.

The characteristic 1/f frequency dependence of the noise power due to these fluctuations is the result of assuming that electron tunneling is the mechanism by which bulk electrons are released from the surface traps. The surface layer is assumed to have some finite thickness and the traps are assumed to be uniformly distributed over this thickness. The tunneling probability depends exponentially on the distance over which tunneling must occur. Consequently, a distribution of lifetimes is obtained which leads to the characteristic 1/f frequency dependence for the noise power.

More quantitatively, this model predicts the following expression[6] for the 1/f noise voltage:

$$v_{1/f} = \left(\frac{N_T}{\alpha}\,\frac{\ell}{w}\right)^{1/2} \frac{E}{2n_o d} \left(\frac{\Delta f}{f}\right)^{1/2} \qquad (3.17)$$

where:

N_T = concentration of traps in the surface layer.

α = characteristic tunneling constant.

PCF

CLASSIFICATION (If Any)

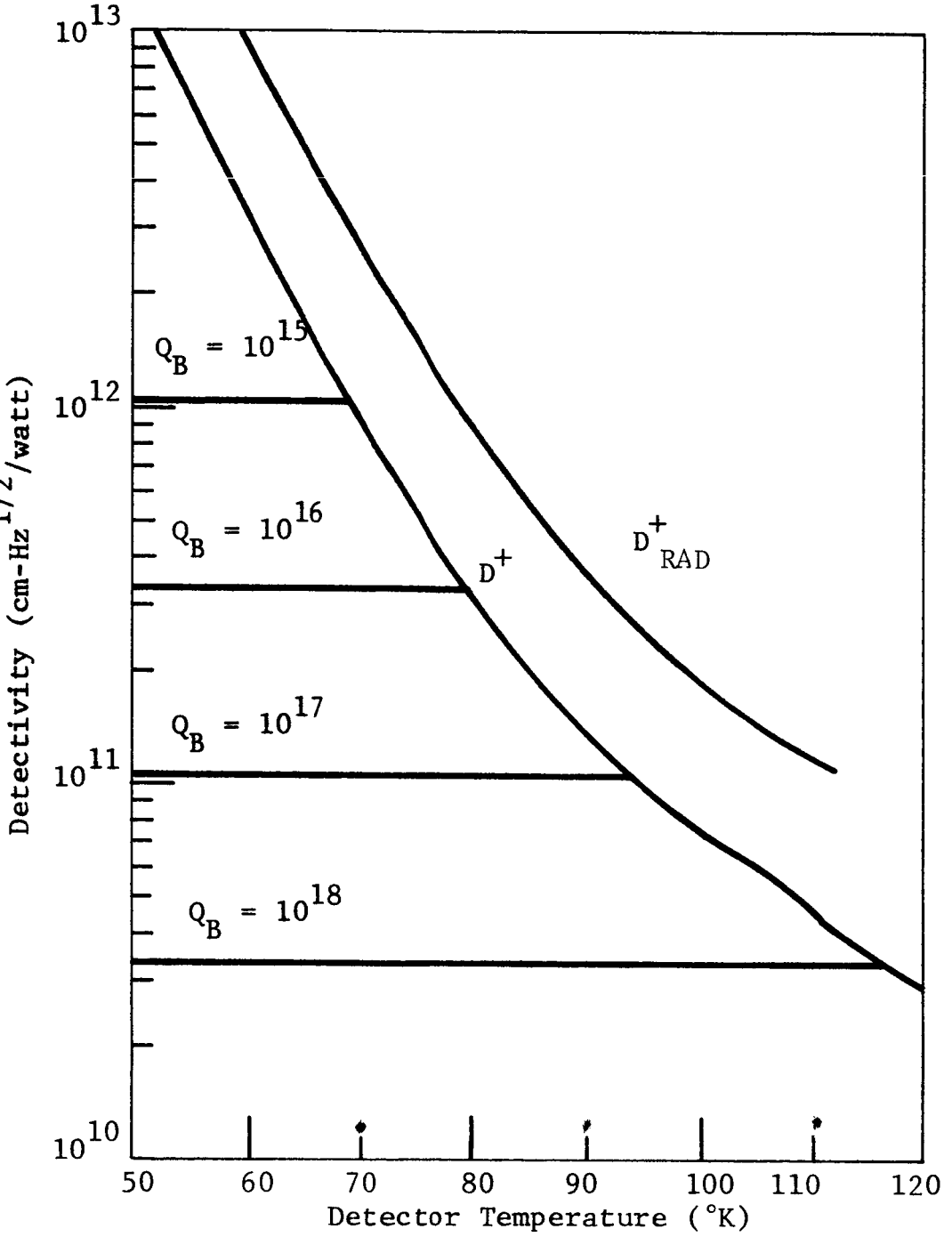

Figure 3.1 DETECTIVITY VERSUS TEMPERATURE AND BACKGROUND FOR 13 MICRON (Hg,Cd)Te DETECTOR

ℓ = sample length (interelectrode spacing).

w = sample width.

d = sample thickness.

E = dc electric field.

n_o = bulk electron concentration

Δf = noise bandwidth.

f = measurement frequency.

This equation can be compared with the definition of the 1/f noise coefficient C_1 and the following expression can be obtained.

$$C_1 = \frac{N_T}{4\, n_o^2}\ \frac{1}{\alpha d} \tag{3.18}$$

Here the coefficient C_1 is explicitly expressed as a function of various material parameters. In particular, C_1 here depends inversely on the sample thickness d. This is due to the surface nature of McWhorter's model. For a bulk 1/f noise mechanism C_1 would be independent of sample dimensions.

Previous work[4,7] showed that C_1 in n-type (Hg,Cd)Te is approximately proportional to $\rho^{5/2}$, where ρ is the sample resistivity; i.e.,

$$C_1 \sim (1/n_o\ e\ \mu)^{5/2} \tag{3.19}$$

where e is the electron charge and μ is the electron mobility. This empirical dependence on carrier concentration is close to that predicted by equation 3.18. However, it must be kept in mind that the electron mobility μ may itself depend on electron concentration.

3.4 HOOGE'S BULK MODEL FOR 1/f NOISE

Based on 1/f noise data for a variety of semiconductors, Hooge has recently proposed that 1/f noise is a bulk phenomenon. He arrived at the following empirical expression for the mean square 1/f noise voltage:

$$v_{1/f}^2 = C\, V^2\, \frac{\Delta f}{f} \tag{3.20}$$

CLASSIFICATION OF ARMY

where V is the dc bias voltage and C is an empirical coefficient given by:

$$C = 2 \times 10^{-3}/N_{tot} \tag{3.21}$$

where $N_{tot} = (n_o \ \ell \ w \ d)$ is the total number of carriers in the sample. A comparison of equations 3.12 and 3.13 with the definition of C_1 gives the following results:

$$C_1 = \frac{2 \times 10^{-3}}{n_o} \tag{3.22}$$

This result for C_1 has a different dependence on carrier concentration than the empirical relation for (Hg,Cd)Te in equation 3.18. However, the mobility also appears in equation 3.18 and contributes an additional dependence on carrier concentration.

PCF

CLASSIFICATION (If Any)

CLASSIFICATION (If Any)

SECTION 4

EARLY EXPERIMENTAL CORRELATIONS

Earlier studies [4,7] of 1/f noise in (Hg,Cd)Te detectors at the Radiation Center showed that the 1/f noise coefficient C_1 varied approximately as the detector resistivity to the 5/2 power for resistivities below about 0.5 ohm-cm. For higher resistivities there was apparently no correlation of C_1 with resistivity. This behavior is shown in Figures 4 and 41 of Reference 4.

Originally it was assumed that all these data were for detectors fabricated from n-type material. After the differences between n-type material and lightly-doped p-type material with a surface inversion layer were established[9], however, it was realized that the data points for resistivities below about 0.5 ohm-cm probably corresponded to n-type samples while those for higher resistivities corresponded to lightly-doped p-type samples. On this basis the correlation of C_1 with resistivity was valid only for n-type material.

In the earlier stages of this program (Phase I--See Introduction) it was attempted to determine which of the above two models was in better agreement with the experimental correlation of C_1 with resistivities in n-type (Hg,Cd)Te. Mobility dependences were determined from the work of Scott[10]. The results of this comparison are presented in Figure 4.1, which shows the data plotted in the form of the square root of C_1 versus electron concentration n_o. All of the available data points are shown, including those for samples known to be lightly-doped p-type. The data points for samples known to be n-type occur for carrier concentrations above about 5×10^{14} cm^{-3} and show that C_1 decreases with increasing carrier concentration. The dashed line in Figure 4.1 is a plot of equation 3.22. Since there are no adjustable parameters in this expression, the order of magnitude agreement is surprisingly good. However, the data fall off more rapidly with increasing carrier concentration than predicted by equation 3.22.

A better agreement for the dependence on carrier concentration is obtained with the solid line, which represents the n_o^{-2} dependence of C_1 in McWhorter's surface model. Both the parameters N_T and α appearing in equation 3.18 are unknown, and furthermore the data are for various thicknesses. Consequently, quantitative agreement with this model is not possible. However, on the basis of the dependence on carrier concentration, this model appears to be closer.

PCF

CLASSIFICATION (If Any)

DO NOT REPRODUCE

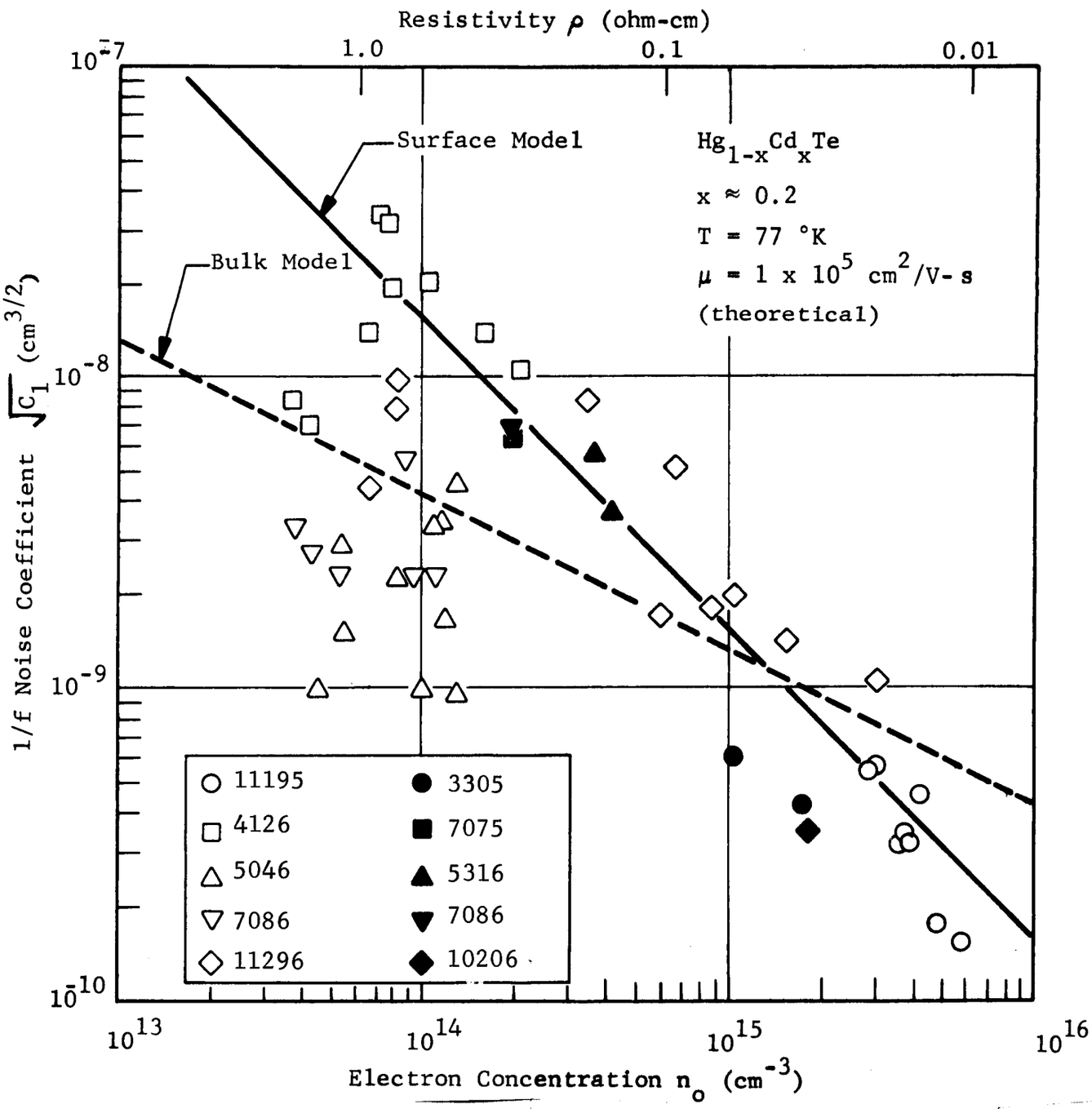

Figure 4.1 SQUARE ROOT OF THE 1/f NOISE COEFFICIENT C_1 VS CARRIER CONCENTRATION. THE SOLID LINE CORRESPONDS TO McWHORTER'S SURFACE MODEL WHILE THE DASHED LINE REPRESENTS HOOGE'S BULK MODEL. (BASED ON DATA OF REFERENCE 10)

CLASSIFICATION (If Any)

These results lead to the conclusion that 1/f noise in (Hg,Cd)Te detectors is by and large typical of much of the results reported in the literature for many types of devices: Considerable variability of the magnitude of C_1 is found, with a decreasing dependence on carrier concentration. For devices of any complexity, no definite correlation with theory has been found, either for specific magnitude, or for dimensional dependences. Hence, new approaches were called for.

PCF

CLASSIFICATION (If Any)

DO NOT TYPE [illegible] SOLID LINES

TYPE
PROOF
CORR
CKD

CLASSIFICATION (If Any)

SECTION 5

NEW APPROACHES

It is important to recognize that before beginning the program, optimism existed for eventual success in reduction of 1/f noise, since specific (Hg,Cd)Te detectors with low 1/f noise had been fabricated. For example, Figure 5.1 shows the noise spectra for detector 10168161C7, which had a value of $C_1 \tilde{\sim} 5 \times 10^{-21}$ cm^3, one of the lowest to date. Note that f_c for this device was about 350 Hz.

The results of the earlier work in the program, and recent theoretical developments indicated directions for fundamental new approaches (these were determined during Phases II and II--See Introduction) Specifically, conclusions were:

1. Studies of 1/f noise in (Hg,Cd)Te should be confined exclusively to n-type material. It is only n-type (Hg,Cd)Te for which the electrical and photoconductive properties are sufficiently well understood to enable a quantitative comparison of detector performance with material properties.

2. Field Effect measurements[11] on silicon had shown a direct correlation between surface properties and 1/f noise. Whether or not one accepts the oxide tunneling mechanism proposed by Fu and Sah[11] to explain their results, it is clear that the significance of the surface has been demonstrated in general.

3. The existence of extensive available data suggested the possibility for productive analysis.

   In recent months HRC had instituted procedures for routinely obtaining noise spectra from a wide variety of completed detectors. In addition, improved understanding and routine material growth and better methods for more relevant Hall and resistivity data had been developed. This new data provided an abundance of useful information for relating 1/f noise to basic material and processing parameters, since a full complement of the pertinent information as available for well categorized material. Parameters, such as responsivity, bias dependence, ambient and thermal effects and other processing variables could be correlated with noise spectra.

CLASSIFICATION (If Any)

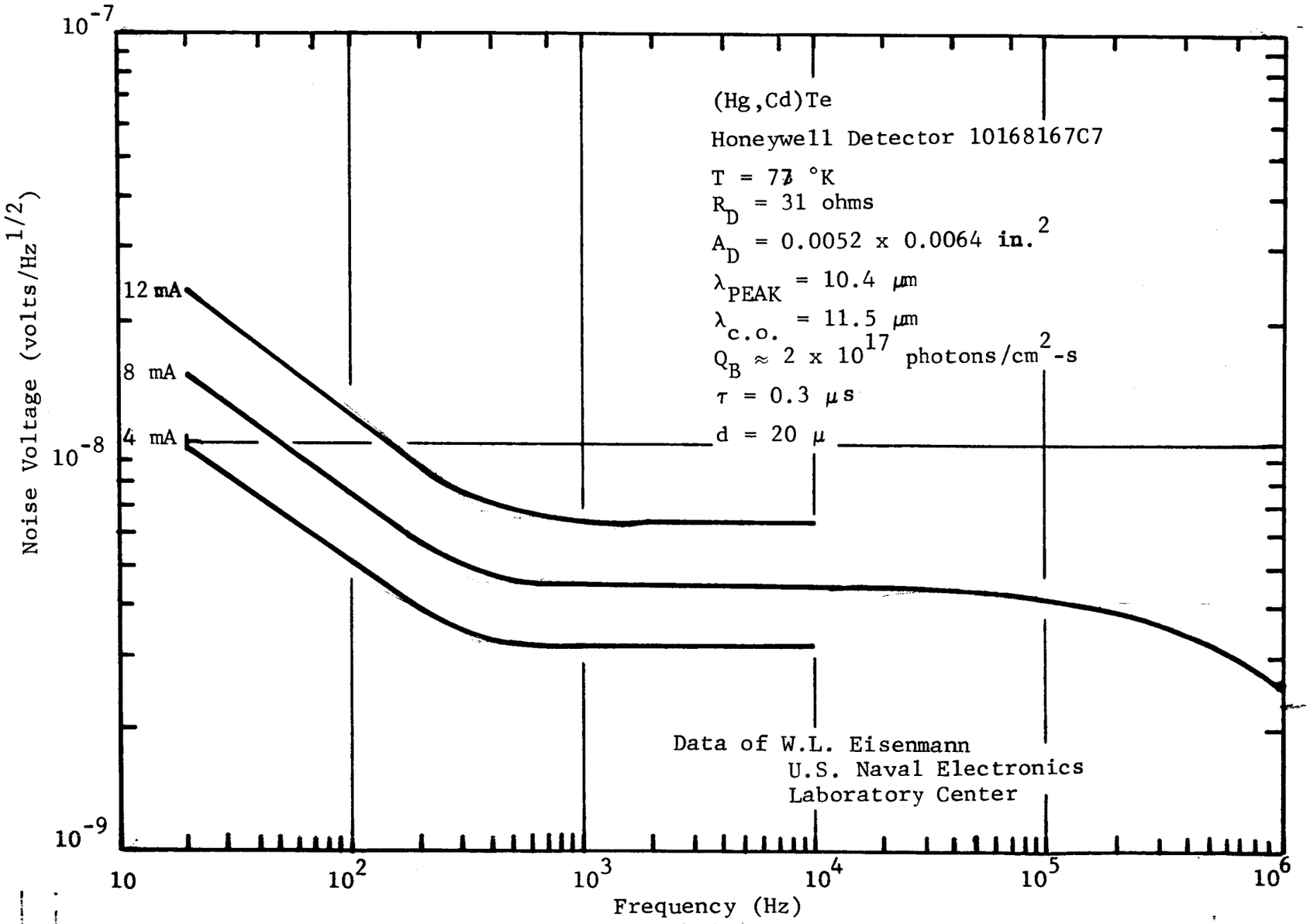

Figure 5.1 NOISE VOLTAGE PER ROOT HERTZ VS FREQUENCY FOR DETECTOR 10168167C7

Therefore, a survey and analysis of this information was initiated at the beginning of Phase IV.

4. New theoretical approaches were under consideration.

S. Teitler and M.F.M. Osborne[12,13] had developed some fairly sophisticated arguments which point out the universal nature of 1/f noise in current-carrying conductors. These arguments dispel much of the mystery about the origin of 1/f noise, especially concerning the occurrence of this noise in a wide variety of conductors and the many mechanisms which have been proposed to account for the phenomenon.

The essential results of these theoretical arguments [12,13] is that 1/f noise results from dissipation of energy, introduced into the conductor at zero frequency by the dc current, by means of a nonlinear process. The nonlinear process couples the energy dissipation to higher frequencies, and the fluctuations associated with the non-dc energy dissipation lead to a 1/f noise spectrum.

A nonlinear process in this context is one which introduces nonlinear terms into the dynamical equation for current flow or particle velocity. Such terms can arise from a nonlinear scattering process or possibly from nonparabolicity in the energy band. In fact, Handel[14] has shown that the magnetic field term in the Lorentz force expression can lead to nonlinearities of the type required to produce 1/f noise.

The picture to emerge, then, is that the 1/f noise observed in a given conductor can be due to any one of a variety of possible mechanisms which lead to nonlinear energy dissipation. Probably one of these mechanisms will be dominant over the others. If the dominant mechanism is connected with the nature of the surface, the contacts or the bulk impurity content, then suitable experiments could be performed to demonstrate this connection and possibly to eliminate the 1/f noise due to this mechanism.

TYPE
PROOF
COPY
CKD

5. Suggested Directions

In view of the above considerations, it was decided to develop procedures with the point of view that the uniformity and linearity of current flow should be increased; with strong emphasis on surface-related effects. Therefore, attention was to be concentrated on control of depletion and inversion surface space charge layers.

CLASSIFICATION (If Any)

SECTION 6

NEW PHENOMENOLOGICAL THEORY

A significant new observation was made concerning 1/f noise in (Hg,Cd)Te detectors. It enabled the determination of a useful phenomenological expression for 1/f noise. Radically different approaches to reduction of 1/f noise were suggested.

The discovery was arrived at as the result of the planned survey and analysis of recently available data from a large number of (Hg,Cd)Te detectors. Specifically, within recent years the product line department has been routinely measuring frequency response of the noise voltage of many detectors. Consideration of this and other data led to the remarkable and unexpected conclusion that, in (Hg,Cd)Te detectors, the 1/f noise voltage ($V_{1/f}$) is proportional to the generation-recombination voltage (V_{g-r}). In the initial application, it was found that v_n (the total detector noise - neglecting Johnson noise) is closely approximated by the empirical expression:

$$v_n^2 = v_{g-r}^2 + K_1 v_{g-r}^{2p}(1/f) \qquad (6.1)$$

K_1 is a constant, which can be directly related to the usual 1/f coefficient, C_1; and the empirical constant $p > 1$. Best initial experimental agreement has been found for a value of $p \approx 1.5$. Thus, the 1/f noise alone is given by

$$v_{1/f} = K_1^{1/2}(1/f)^{1/2} v_{g-r}^{3/2} \qquad (6.2)$$

It is to be noted that this empirical relation holds whatever the source of v_{g-r} (probably it is only the recombination noise which determines the effect). In this viewpoint, 1/f noise is "current noise" simply because v_{g-r} varies with the current. Also, 1/f noise decreases inversely with sample resistance simply because v_{g-r} behaves in this manner. The corner frequency, f_c, follows directly from equating v_{g-r} with $v_{1/f}$ from Equation 6.2:

$$f_c = K_1 v_{g-r}^{2(p-1)} \cong K_1 v_{g-r} \qquad (6.3)$$

Equations 6.1 to 6.3 state that 1/f noise increases rapidly with g-r noise. Therefore, everything else being equal, in order to reduce 1/f noise, material with low g-r noise should be selected.

This is exactly opposite to previous criteria, when it was believed that $v_{1/f}$ was independent of v_{g-r} and therefore an increase in v_{g-r} would cover up the 1/f noise. That is, according to previous theory, v_n is given by

$$v_n^2 = v_{g-r}^2 + v_{1/f}^2 \qquad (6.4)$$

Here $v_{1/f}$ is related to v_{g-r} only <u>indirectly</u> via the sample current, I (i.e. $v_{g-r} \propto I$ and $v_{1/f} \propto I$, also).

In terms of detector and material parameters, the effects on 1/f noise can be determined from the well-known expression for the generation-recombination voltage, equation 3.7:

$$v_{g-r} = \frac{2E}{n_o}(\ell/w)^{1/2}(\tau/d)(\eta Q_B + \eta_\ell Q_\ell)^{1/2}(\Delta f)^{1/2} \qquad (3.7)$$

where E is the dc bias field, n_o is the free electron concentration, τ is the photoconductive response time, η is the optical quantum efficiency, Q_B is the incident background photon flux, and η_ℓ and Q_ℓ are analagous terms referring to lattice-induced electron-hole pair generation. From this viewpoint, considering Equation 6.3, the following criteria for the reduction of the effects of 1/f noise can be established:

1. Use lowest feasible bias current.
2. Keep detector temperature below thermal generation range.
3. Reduce detector background as far as possible.
4. Choose semiconductor material with large donor concentration.
5. Develop improved processing methods (to reduce K_1).

An example of the application of Equation 6.1 to experimental data is shown in Figure 6.1. (In fact, it was observation of such data that led to the recognition of the effect.) The curves in the figure represent detector noise voltage, v_n, calculated from Equation 6.2 with p = 1.5:

$$v_n = v_{g-r}(1 + K_1 v_{g-r}/f)^{1/2} \qquad (6.5)$$

PCF

DO NOT TYPE BELOW SOLID LINES

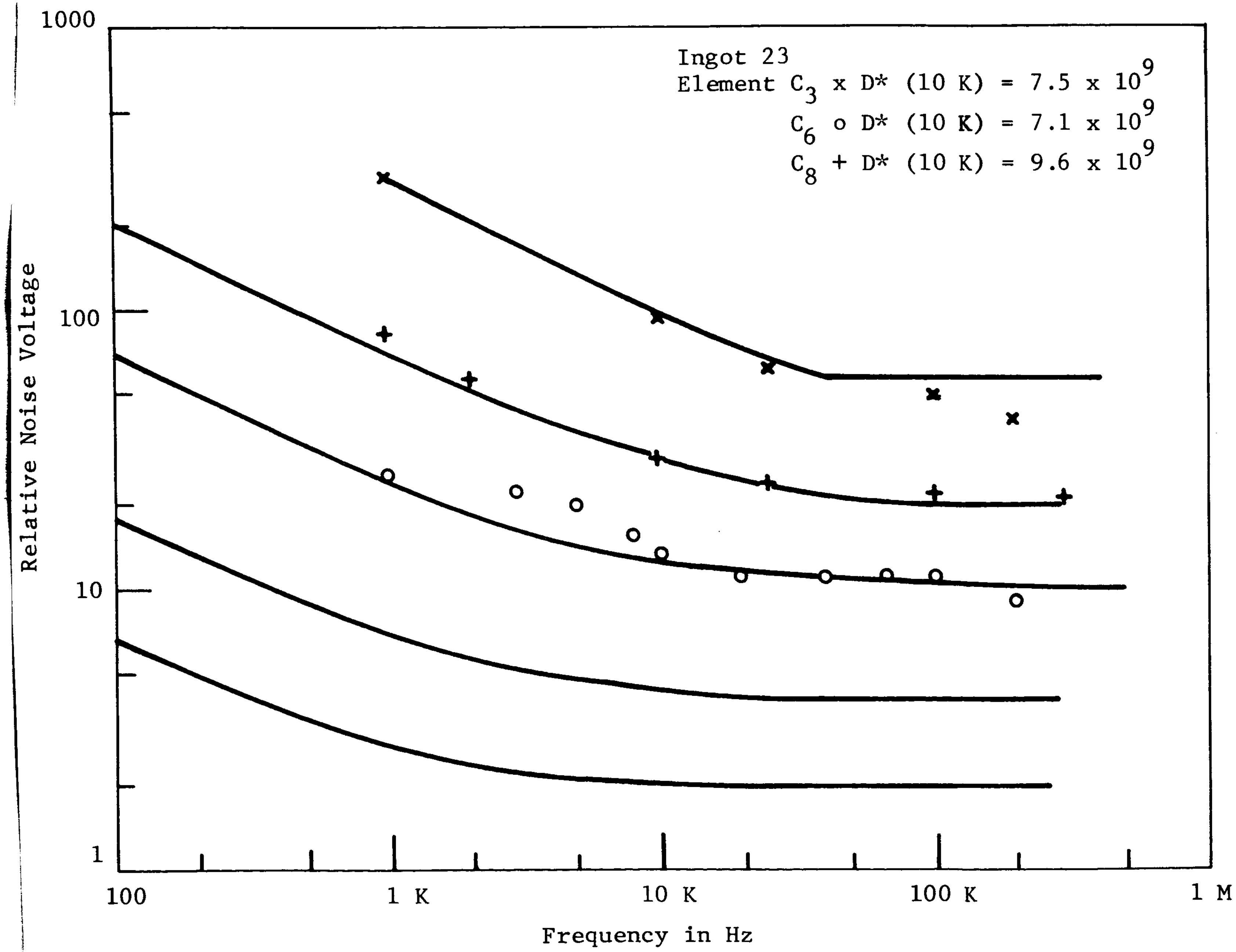

Figure 6.1 NOISE SPECTRUM FOR THREE DETECTORS

The data points represent measured values of noise voltage on three detectors fabricated from similar material. Although widely varying in v_{g-r}, the value of D^*_{BB} is not greatly different from element to element. Note the close correspondence between experiment and empirical theory.

This result has important implications for reduced background operation, since v_{g-r} depends on background as shown in Equation 3.7. In fact, reduction of 1/f noise with background was observed a number of years ago at Honeywell, although information was not available concerning the extent of the effect nor concerning relations to other detector measurements. The result of this observation is shown in Figure 6.2, which is taken from an internal Honeywell Radiation Center report written by L.C. White and T. Koehler.

Similar effects have also been observed on recently prepared samples which were investigated to substantiate the observation. Essentially, results were obtained similar to those shown in Figures 6.1 and 6.2, and consistent with equations 6.1-6.3. Figure 6.3 shows the background dependence of f_c for high performance detectors.

It should be emphasized that criteria 1-4 for reduction of 1/f noise are determined by the observed phenomenology of 1/f noise. Where low frequency operation is contemplated, they should be implemented wherever possible. Further reduction of low frequency noise must come from reduction of K_1 by material and processing technology development.

If we maintain the nonlinearity viewpoint of Teitler and Osborne, the observed g-r noise - 1/f noise correlation leads to an interesting viewpoint since one is thereby led directly to the consideration that 1/f noise originates in nonlinearities in the g-r process. Now the generation mechanism can be eliminated as a source of nonlinearity since 1/f noise is found both for thermal and optical generation. Therefore, we are led to the working hypothesis that 1/f noise originates in nonlinearities in the recombination process. These nonlinearities can be manifested in contact, volume, or surface irregularities – to the extent that they influence the recombination of carriers. Therefore, reduction of 1/f noise in (Hg,Cd)Te requires concentration on minority carrier recombination. In this context, it appears desirable to develop processes to increase the uniformity of current flow by control of depletion and inversion layers, since carrier recombination is strongly affected by these phenomena.

ATION (If Any)

TYPE
PROOF
CORR
CRD

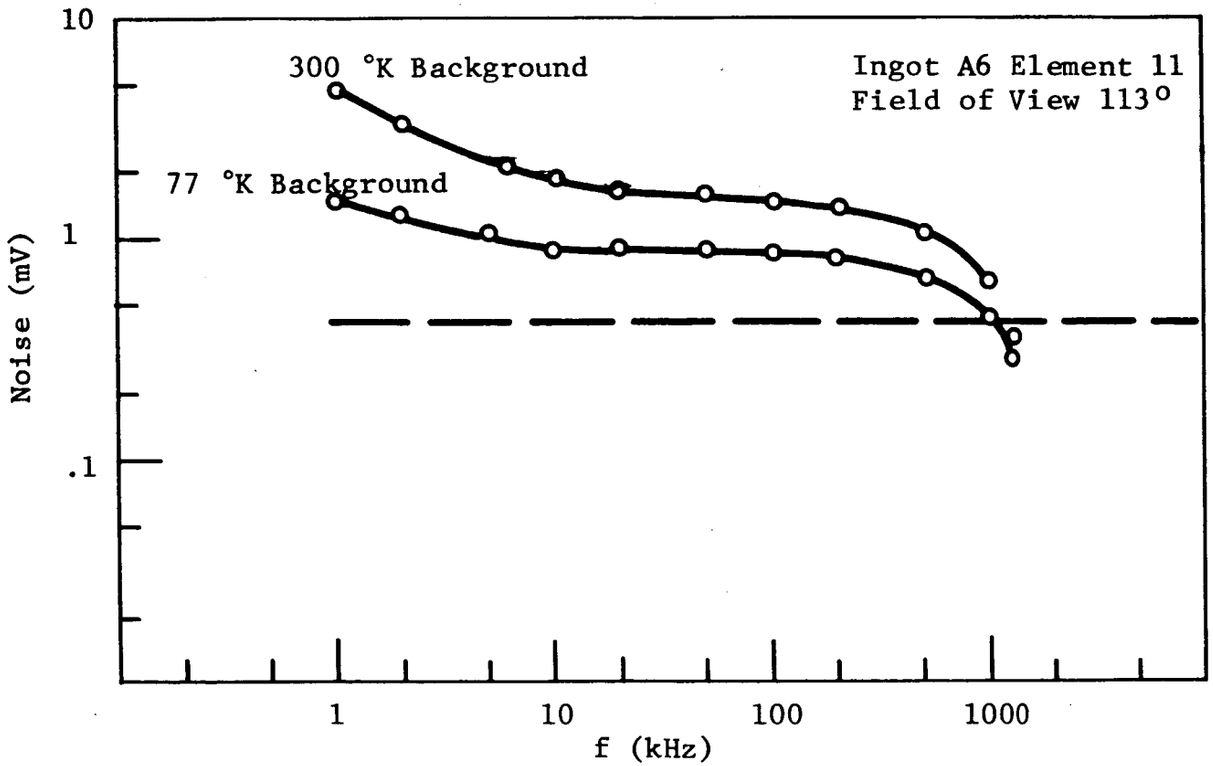

Figure 6.2 NOISE SPECTRUM VS BACKGROUND

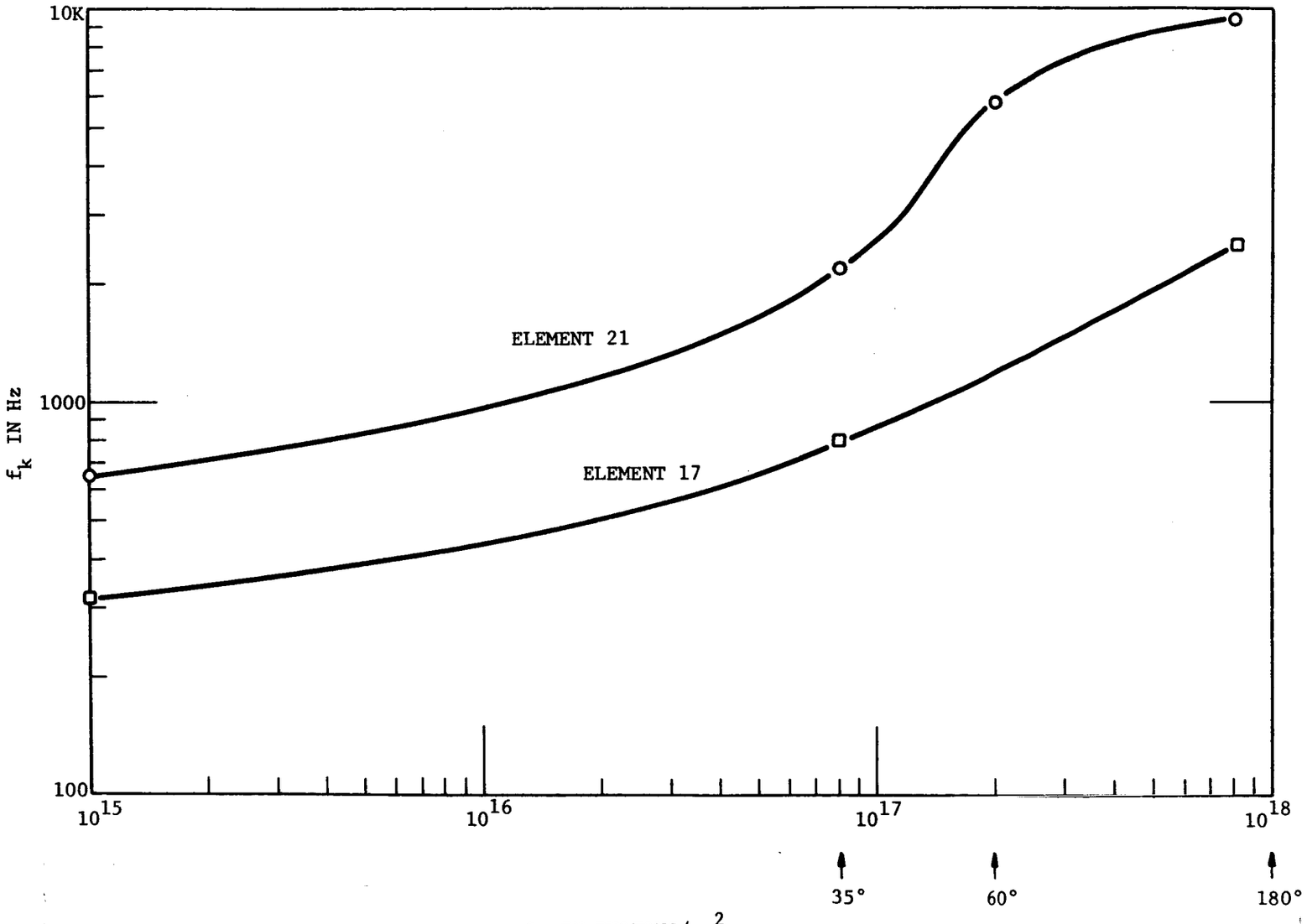

Figure 6.3 1/f KNEE VS BACKGROUND

CLASSIFICATION (If Any)

SECTION 7

SPECIAL EXPERIMENTAL TECHNIQUES - SURFACES AND VOLUMES

In order to evaluate the influence of fabrication procedures, it was necessary to develop special experimental techniques.

Detector processing usually begins by cutting ingots of the material into slabs. Detectors are then made from the slabs by a number of procedures including: thickness reduction, mounting of the thinned material, delineation of elements, and provision of contacts. Thus the usual detector process requires that the (Hg,Cd)Te be bonded to an inert substrate, and then be polished and etched down to a thickness of about 10-30 microns. The material then becomes too thin and delicate for further handling and therefore must remain bonded to the substrate. Approximately half of the surface area (the bonded area) becomes inaccessible to treatment. Moreover, the bonding agent cannot withstand the treatment temperatures contemplated for some of the experiments. Therefore, a method for evaluation of the effect of surface preparation procedures was required with the following special properties: (1) isolation of surface from volume effects; (2) elimination of back surface effects; (3) non-destructive evaluation of the slab. In sum, it was required to evaluate detector noise behavior without actually fabricating detectors.

For this purpose, we developed arrangements which would allow one to work with special evaporation patterns on top of thick slabs, or bulk material, so that permanent bonding is not required, and only the top surface is operant. Two types of special electrode configurations were developed. For one type ("parallel plates"), both contacts are in close proximity on the top surface. When data from parallel plates are properly obtained and analyzed, they permit the determination of surface effects on 1/f noise. The second configuration consists of isolated circular dots of varying diameter evaporated on the top surface. Data from dots permits the determination of the volume contribution to 1/f noise, as well as independent measurement of material resistivity.

Both patterns place special requirements on measurement technique because they inherently have considerably lower resistance than detectors, and therefore generate less noise. This limitation was overcome by providing methods for measurements at lower frequencies in order to enhance the 1/f component of the noise. (In addition, bias levels can be raised somewhat.)

PCF CLASSIFICATION (If Any)

DO NOT TYPE BELOW THIS LINE

7.1 PARALLEL PLATE CONFIGURATION

This structure is in the form of parallel plates which are closely spaced so that an appreciable response is obtained from regions of the order of the thickness of the optical absorption or diffusion length. Electrode material not required for bonding and conduction is removed. The form of this structure is sketched below.

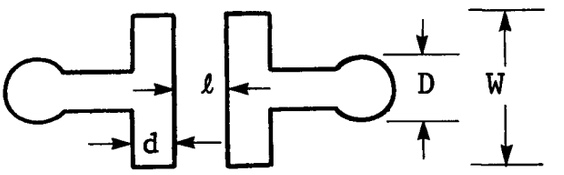

The resultant effect of top slab electrodes can be approximated by the configuration:

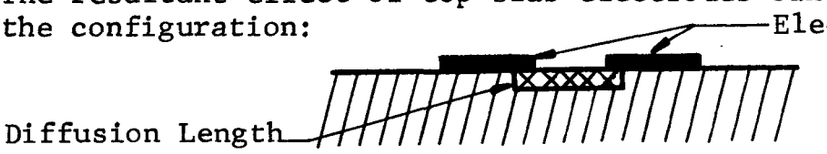

With the equivalent circuit,

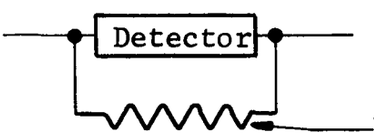

The relative magnitude of the volume shunt can be estimated from the following calculations which were used to evolve and analyze the parallel plate structure. The "surface" conductance is given by

$$\Sigma_s = \sigma W t_s / \ell \qquad (7.1)$$

where σ is the bulk conductivity, and t_s is the effective thickness of the surface layer. The conductance through the volume was roughly estimated by using approximate electrode geometries for closed form solutions from electrostatic theory:

$$\Sigma_v \cong \sigma W \left\{ \frac{1}{\cosh^{-1}\left(\frac{\ell}{d} + 1\right)} + 2\,\frac{D}{W} + \frac{\pi (L/W)}{2\ell n^2 (L/b)^{1/2}} \right\} \qquad (7.2)$$

The first term originates from the volume conductance of the parallel electrodes, the second from that of the circular contacts, and the third from that of the connecting leads. Placing the actual dimensions in the formula, we obtain

$$\Sigma_v \approx \sigma W\ (.77 + 1 + .59) \cong 2.4\ W \sigma \qquad (7.3)$$

PCF
CLASSIFICATION (If Any)
DO NOT TYPE BEYOND SC

Thus the surface-to-volume ratio is

$$\rho_{SV}^{c} \cong \Sigma_s/\Sigma_v \sim \frac{1}{2.4}\frac{t}{\ell} \tag{7.4}$$

But the surface-to-volume conductance ratio of a detector of thickness, t, is given by

$$\rho_{SV}^{d} \cong \left.\frac{\Sigma_s}{\Sigma_v}\right|_{\text{thin detector}} = \frac{t_s}{t} \tag{7.5}$$

Thus, the relative surface-to-volume ratios for the two configurations are given by

$$\frac{\rho_{SV}^{c}}{\rho_{SV}^{d}} = \frac{1}{2.4}\frac{t}{\ell} \tag{7.6}$$

For the purpose of reducing this ratio, ℓ is made small (ℓ =.001" $\approx$ 1.25t - - other electrode designs were for ℓ=.0018"). Thus

$$\frac{\rho_{SV}^{c}}{\rho_{SV}^{d}} \sim \text{O.M.}\ \frac{1}{3}$$

The actual value, determined experimentally, was found to be close to this ratio. Hence, the analysis predicted, and the experiments verified, the feasibility of this technique.

7.2 DOT CONFIGURATION

In addition to the parallel plate configuration, a second type of element was also included in the mask design. The parallel plate configuration was designed essentially to monitor the top surface with reduced influence from the volume. It is also useful and desirable to determine volume effects with reduced influence from the surface. For this purpose, we utilized the "dot configuration", which takes the form of evaporated circles, of differring diameters, on the surface.

PCF [redacted] (...ON If Any)

DO NOT TYPE BELOW ...

The dots relate directly to the "spreading resistance" technique, which can be used to measure volume resistivity. The resistance to the dot, R_S, is given by

$$R_S = \rho/2D \qquad (7.7)$$

where ρ is the volume resistivity and D the diameter of the contact. Measurements to these dots (of diameters 0.002 inch, 0.005 inch, and 0.008 inch) are useful for several purposes: (1) contact anomalies can be demonstrated — if contacts are good then R_S varies as D^{-1} only, (2) volume resistivity can be measured; therefore, the whole process can be checked out by comparison with independently obtained values of resistivity, and (3) the magnitude of volume generated 1/f noise can be estimated since most current flow to the dots originates in the volume.

SECTION 8

MEASUREMENT METHODS

8.1 SPECIAL REQUIREMENTS

The slab isolation technique requires measurements on low resistances at low frequencies (below 100 Hz); therefore special problems arise.

Analysis of initial experimental results indicated the existence of experimental difficulties with the usual equipment. Noise characteristics were observed increasing more sharply than 1/f at frequencies below 100 Hz. It was established that the results were anomalous. Moreover, considerable variation in noise magnitude was observed from element to element. Therefore a complete redesign was performed on all experimental techniques, taking account of the many unique problems that can appear when measuring noise voltages below 100 Hz.

Three requirements are involved: (1) the detector must be dc biased, (2) amplification of the noise voltage is necessary, and (3) accurate measurements are needed of the amplified noise.

8.2 DETECTOR BIAS

A special bias supply was designed and constructed. A number of sources of undesired low frequency noise occured in the current delivery mechanism. They were either reduced or eliminated. They include:

a. Resistors dissipating more than 25% of their power rating should not be used.

b. Noisy batteries - Wet cells and mercury cells were not satisfactory. Many dry cells also were noisy below 100 Hz. A reasonably satisfactory source was found to be two Burgess Type 5308 batteries in parallel.

c. Poor connections of all types - Clip leads cannot be used; wires are now soldered to external pins. Every connector must be inspected and chosen for solid, stable low resistance contacts.

d. Thermal emf's must be reduced. Although they are not current-dependent, they can add to system noise.

DO NOT TYPE BELOW THIS LINE

e. Low frequency fluctuations in ambient light can add a spurious noise source.

8.3 AMPLIFIER

The standard amplifier, although providing valid results, was not completely satisfactory in that the gain was too low and was also dependent on the detector resistance. (This was calibrated for, but was still inconvenient.) Therefore, a new amplifier with higher and uniform gain was designed and constructed by modifying a standard Honeywell preamplifier module for low frequency operation and adding a standard ac coupled op-amp as a post amplifier.

8.4 MEASURING APPARATUS

It was established that the Quan-tech type 304 TDL wave analyzer, which has been used to date, is a very satisfactory measuring instrument for these applications. Its usefulness was improved by reading out the noise signal on an x-y recorder. The frequency sweep feature of the Quan-tech analyzer permitted direct readout of noise voltage vs frequency. The combination of visible recorder fluctuations and proper analyzer time constant (10 seconds for 1 Hz bw) provides accurate statistical results.

PCF

CLASSIFICATION (If Any)

DO NOT TYPE BEYOND SCALE

TYPE
PROOF
CORR
RCD

CLASSIFICATION (If Any)

SECTION 9

LOW FREQUENCY ANOMALIES

It is useful to report the results of low frequency measurements that were proved to be anomalous, since data of this type can be misinterpreted as an indication of detector performance. It was found that most experimental anomalies would introduce apparent large low frequency voltages increasing more rapidly than the first power of inverse frequency.

9.1 CONTACT EFFECTS — 1/f NOISE FROM CONTACTS

Initial results on top surface noise were erratic and unsatisfactory:

a. Both dot and parallel plate resistances were generally higher than would be expected from known values of resistivity.

b. The dot resistances did not vary inversely with dot diameter, as required by spreading resistance theory.

c. Measured 1/f noise was much larger than should have been observed, especially on the dots, which should respond mainly to volume properties.

d. Both resistance and noise values were erratic on many elements.

Straightforward experiment and analysis allowed us to establish that the problem originated in the thermocompression bonds used to make contact to the elements. It is generally recognized that the thermocompression bond, required for mechanical strength in detector fabrication, does indeed cause considerable material damage, and that these bonds must be isolated from the active detector area, or poor performance and high 1/f noise will result. What we had not anticipated, however, was the extend and depth of damage. It had been hoped that proper isolation and the use of large indium dots and pads on both types of elements would eliminate contact damage problems. But these precautions proved to be insufficient.

For the next set of experiments, the first set of contacts were etched away, the slabs fabricated as before, and extra thick indium elements were evaporated. Contacts to the elements were made

PCF

CLASSIFICATION (If Any)

DO NOT TYPE BELOW THIS LINE

OF

by minimal light mechanical pressure from bonding wire to indium pad. The data from these elements was much more reasonable and stable. Dot and parallel plate resistances were generally of the predicted magnitude, and over much of the experimental slab area, dot resistances did indeed vary inversely with dot diameter.

9.2 OTHER SPURIOUS EFFECTS

The noise characteristics generated by spurious sources, using the non-optimized experimental equipment, data were obtained on four types of samples, all in the resistance range of 3 to 4 ohms:

a. a 3-ohm carbon resistor, for comparison purposes and checkout of the technique;

b. a large thick 3.5-ohm bar of (Hg,Cd)Te, of dimensions ℓ = 0.80 cm, w = 0.215 cm, t = 0.15 cm;

c. dot configurations on the (Hg,Cd)Te slab;

d. parallel plate elements on the (Hg,Cd)Te slab.

Measurements below 100 Hz were made using a 1 Hz bandwidth on the Quan-tech 304TDL wave analyzer. Above 100 Hz, a bandwidth of 10 Hz was used.

Figure 9.1 shows the frequency response of the noise voltage measured on three of the parallel plate elements. Figure 9.2 shows the spectra measured on a 0.005-inch dot and on the thick bar. No measurable 1/f noise at the bias levels investigated was found on the 3-ohm resistor. All data are shown for a bias of 20 mA. Measurements were also taken at 10 mA, and at 0 mA (to determine amplifier noise). The noise voltage increased approximately linearly with current, as expected. The amplifier noise was removed from the data by finding the rms value of the difference between the square of the measured noise and the square of the amplifier (0 bias) noise.

The rising low frequency noise characteristics and the variability of results are anomalous. These effects were eliminated by proper redesign of the experimental apparatus, discussed above.

PCF

DO NOT TYPE BELOW THIS LINE

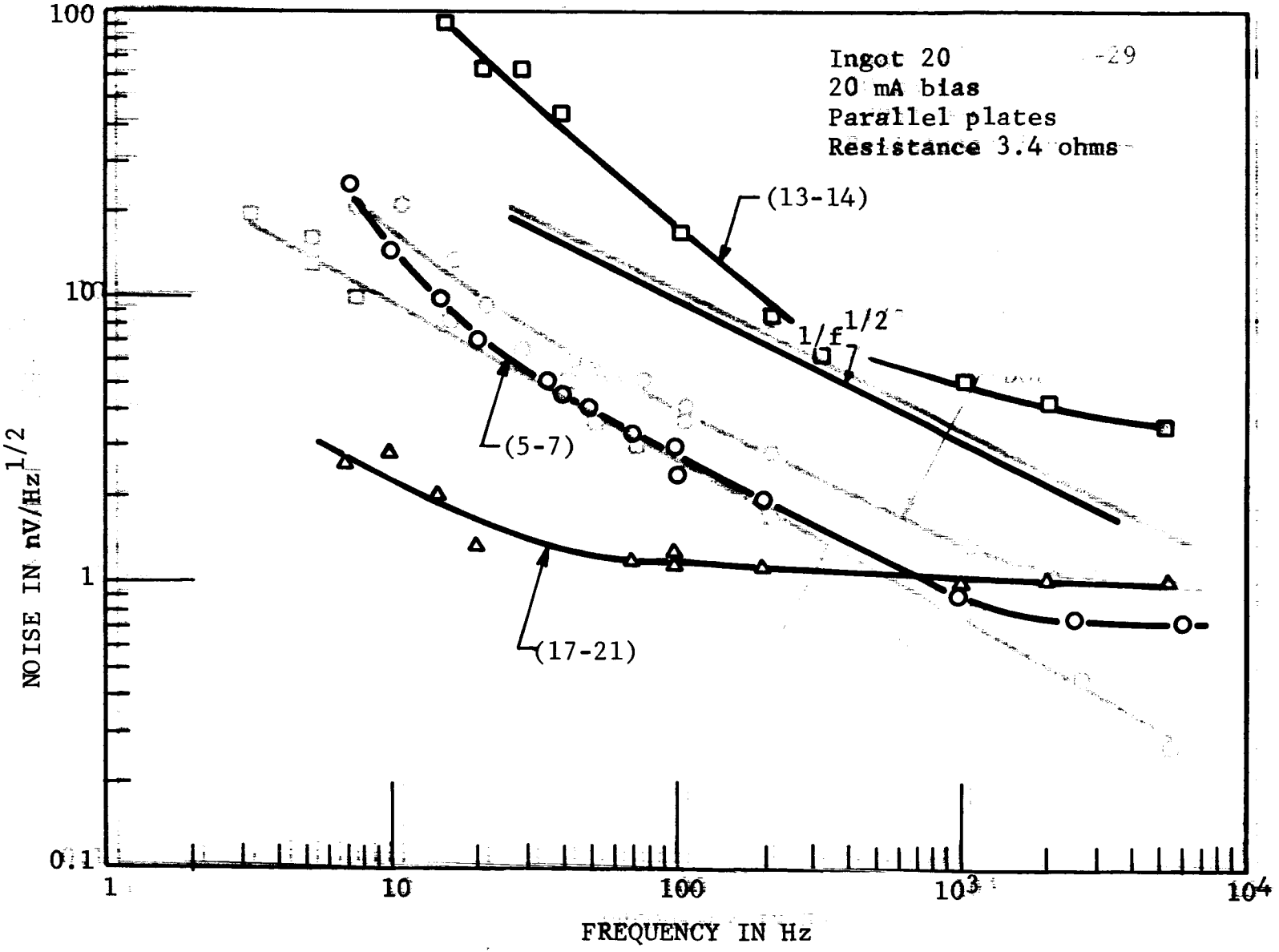

Figure 9.1 ANOMALOUS NOISE vs FREQUENCY FOR PARALLEL PLATES

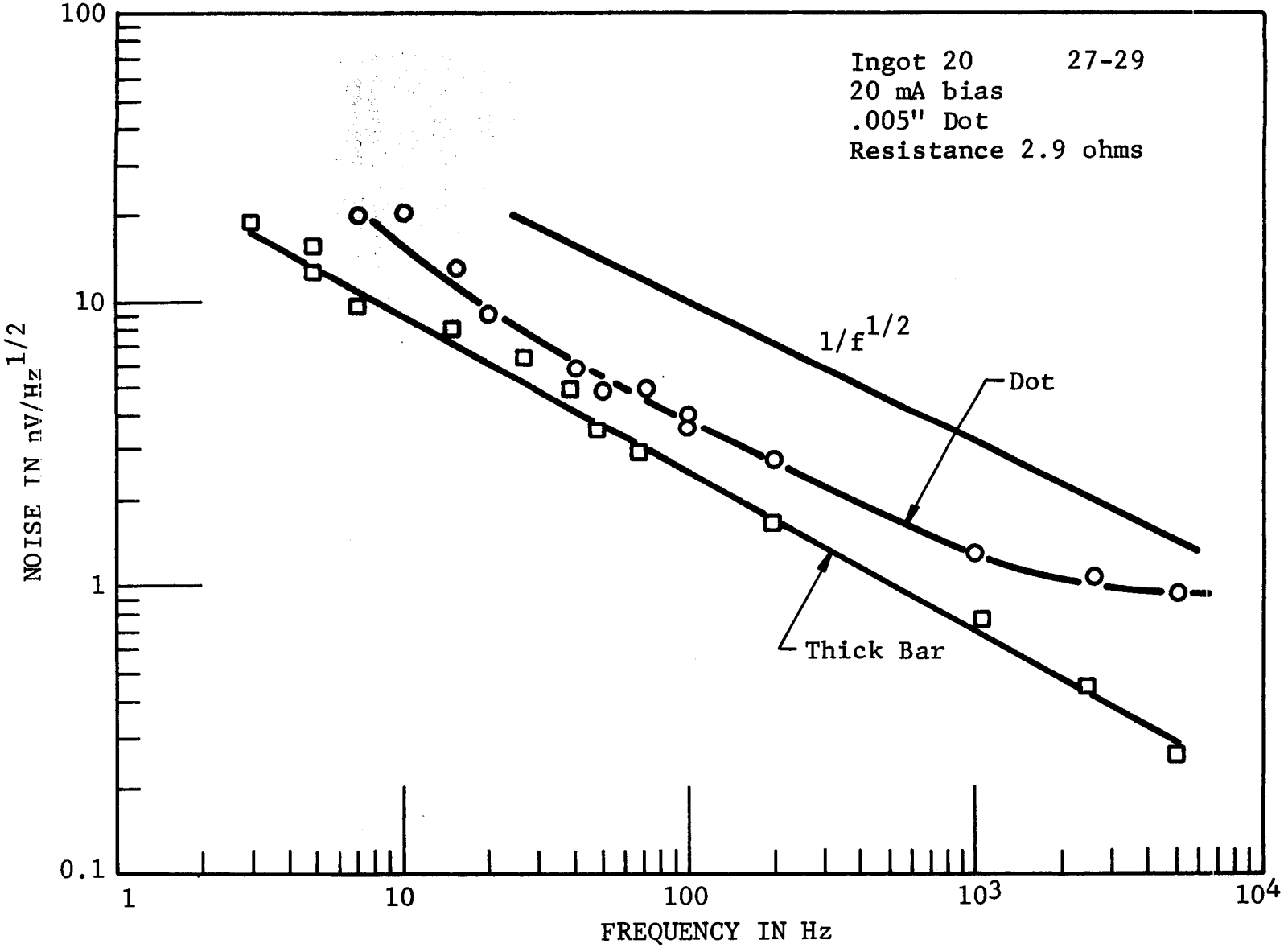

Figure 9.2 ANOMALOUS NOISE vs FREQUENCY FOR MEDIUM DOT AND BAR

SECTION 10

NOISE FROM DOTS--ORIGIN OF 1/f NOISE

10.1 EXPERIMENTAL

10.1.1 Background Generated Noise

Noise frequency spectra were measured on dots of various sizes on several slabs under conditions for which the gr noise was known to be dominated by background illumination. Typical results are shown in Figure 10.1 for dots of two different diameters (3 mil and 5 mil).

The following features of this data should be noted:

a. Considerable 1/f noise is observed for the dot configuration.

b. A nearly linear inverse frequency dependence (of power) is observed. Thus the noise is truly "1/f."

c. The noise voltage varies approximately as the 1.5 power of the dot diameter. This result has been obtained on many dots of various diameters on several slabs. Power dependences were always found to be much less than 2, and to vary from ~1.2 to 1.6 as is shown for some typical results in Figure 10.2.

d. It was important to determine if observed noise from dots would also exhibit the background dependence found on detectors (See Figure 6.3 and Section 6).

   To investigate this, a slab was mounted in a special test chamber which permitted reduction of background from $\sim 8 \times 10^{17}$ photons/cm^2-s down to $\sim 8 \times 10^{16}$ photons/cm^2-s. A large reduction in low frequency noise was indeed observed under these conditions, with the remaining noise just barely measurable above amplifier noise.

CLASSIFICATION (If Any)

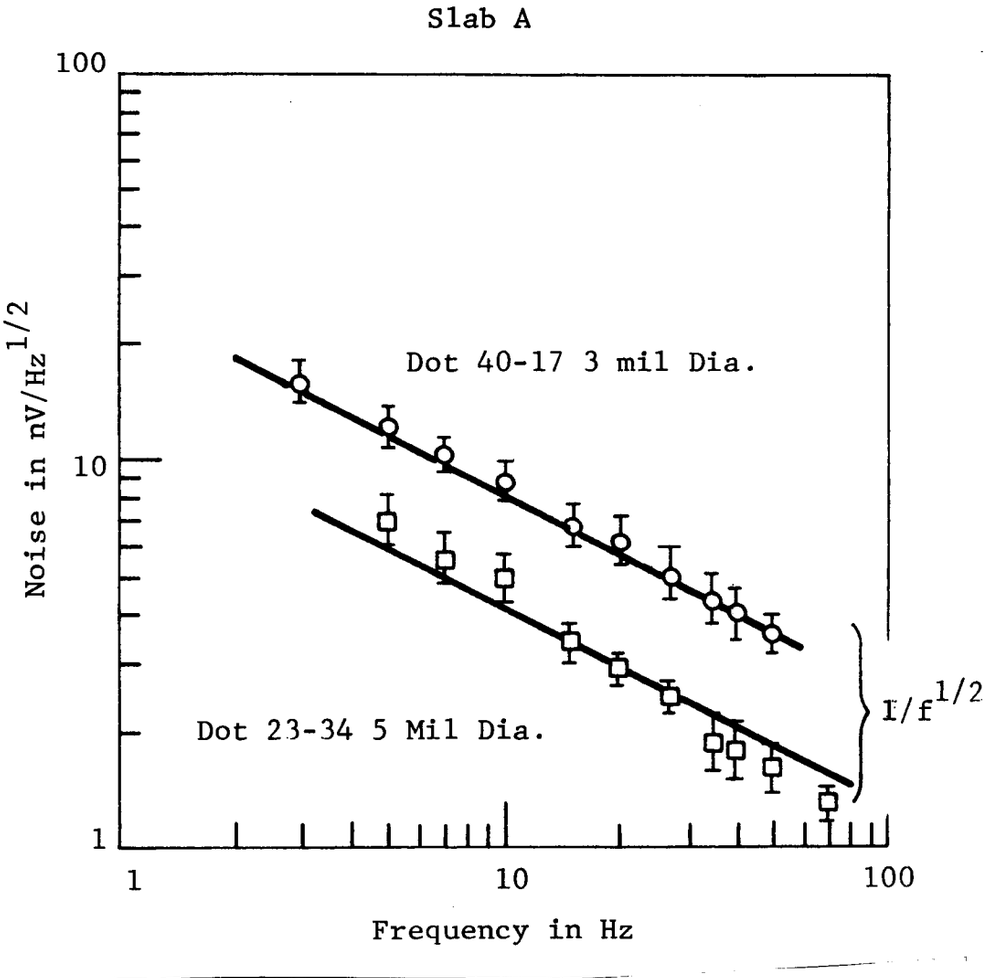

Figure 10.1 NOISE FROM DOTS

CLASSIFICATION (If Any)

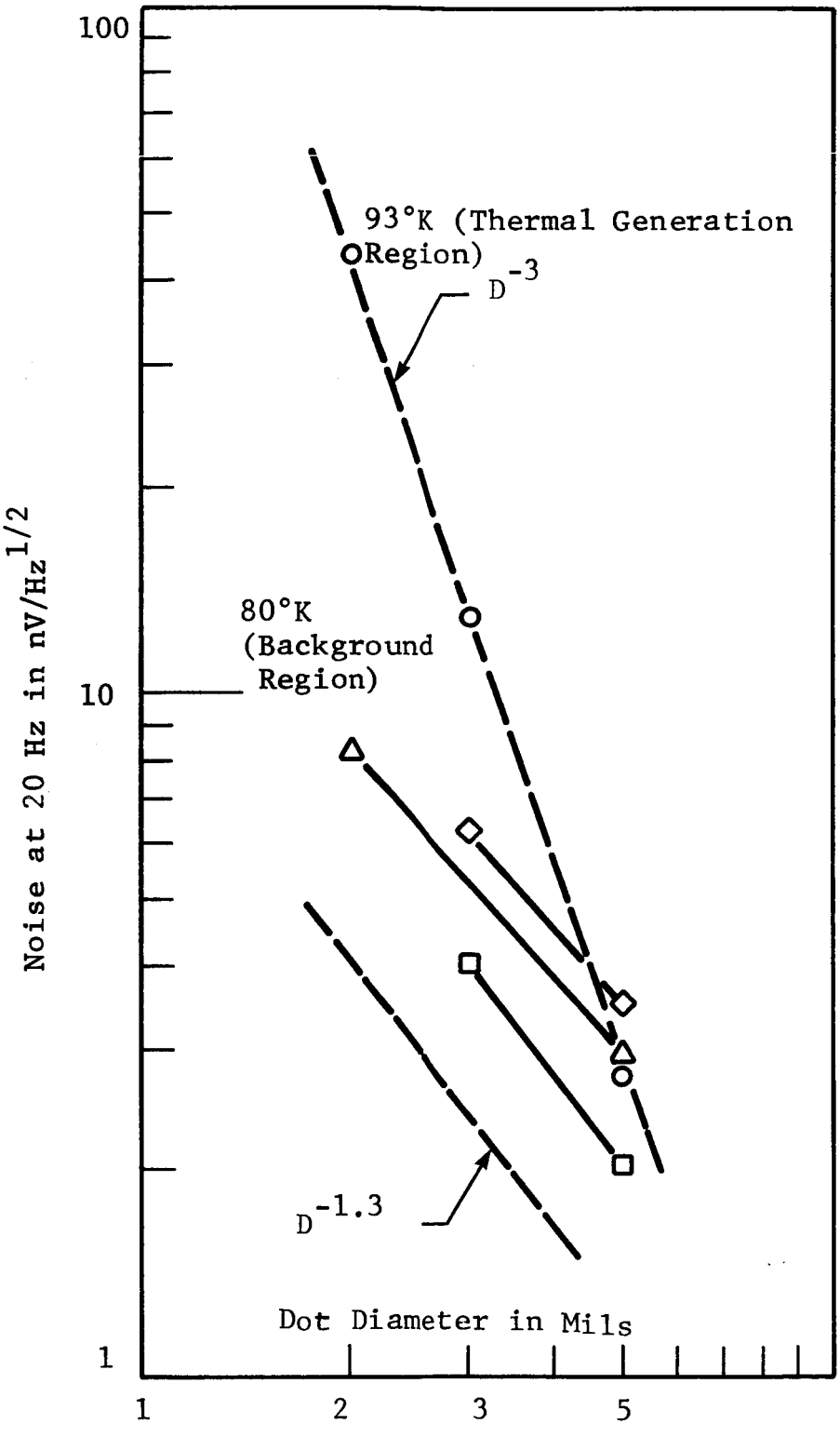

Figure 10.2 1/f NOISE VS DOT DIAMETER

10.1.2 Thermally Generated Noise

According to the analysis below, the dependence of noise on dot diameter provides important information concerning 1/f noise mechanisms. Figure 10.2 shows the experimental results for 1/f noise measured for three different dot diameters on an (HgCd)Te slab which was raised to a temperature of 90°K, where gr noise is known to be dominated by thermal processes.

10.2 DIMENSIONAL ANALYSIS

Results from dots are related to basic noise mechanisms. Specifically, it can be determined whether or not 1/f noise originates at statistically independent sources distributed uniformly throughout the volume, as is well known for other noises, such as g-r noise.

In this, "classical theory" approach, noise is due to conductivity modulation in the volume. Thus local fluctuations in conductivity lead to the appearance of external noise voltages when a dc current is applied.

The purpose of this analysis is to determine the expected dependence of noise on dot diameter for a conductivity modulation mechanism.

We begin by using results derived by Van der Ziel[5] for the noise voltage from a rectangular bar of length L and area A, with resistivity ρ:

$$v_n = K_\rho I L^{1/2}/A^{3/2} \qquad (10.1)$$

We wish to consider three situations:

a. The 1/f noise originates throughout the volume.

b. It originates in a region just under the contact.

c. It originates from a region about the periphery of the dot (probably from diffusing minority carriers generated there.)

Case 1 represents noise generated from the identical volume region responsible for the spreading resistance. For this condition, to a first approximation, the effective length is proportional to the diameter, D. Therefore, $v_n \sim D^{1/2}/D^3 = D^{-5/2}$.

In Case 2, the length will be determined by some physically constant dimension, L_D (possibly some type of diffusion length). Then $v_n \sim L_D^{1/2}/D^3 \sim D^{-3}$.

Case 3 is most readily determined by beginning with the fundamental equations[5] (which also give the same results for cases 1 and 2).

$$\frac{\delta(\Delta V)}{V_o} = \frac{\delta(\Delta N)}{N_o} \quad \text{and} \quad \delta(\Delta N) \sim \Delta N^{1/2} \tag{10.2}$$

$\delta(\Delta V)$ is the noise voltage caused by a fluctuation in the carriers (total carriers in volume) = $\delta(\Delta N)$, with V_o the applied voltage and N_o the <u>total</u> carriers participating. The model for this case is that the operant noise originates from carriers surrounding the dot over a diffusion distance L_D. Thus $\Delta N \cong \pi D L_D^2$, and $\delta(\Delta N) \sim D^{1/2}$; whereas N_o includes all operant carriers participating in the current flow throughout the volume.

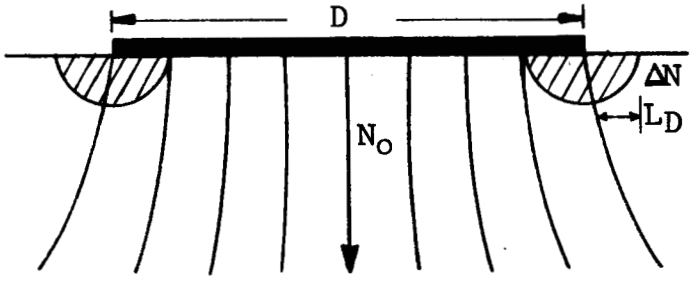

Then $\delta(\Delta V) \sim (V_o/N_o) D^{1/2} = (I_o R_o/N_o) D^{1/2} = \frac{\rho}{D n_o D^3} D^{1/2}$. Thus, the noise $\sim D^{-7/2}$. In sum: (10.3)

1.	volume	$v_n \sim D^{-5/2}$	
2.	volume near dot	$v_n \sim D^{-3}$	(10.4)
3.	surrounding dot	$v_n \sim D^{-7/2}$	

where N_o is the carrier concentration ($N_o \cong N_o D^3$).

10.3 SIGNIFICANCE OF RESULTS - ORIGIN OF 1/f NOISE

According to the results on detectors presented in Section 6, and similar experimental results on dots andparallel plates, 1/f noise is related directly to gr noise.

For the experiment described in 10.1.2, the temperature is high enough that thermal generation predominates, and therefore gr noise is distributed uniformly in the volume. Comparison of the upper curve in Figure 10.2 with the dimensional analyses shows that,

under these conditions, 1/f noise also is distributed randomly and uniformly throughout the volume.

However, when the gr noise is determined by background radiation, at 78°K where thermal generation is negligible, the dependence of 1/f noise on dot diameter is much weaker than predicted by conductivity modulation. Now it is certain that background determined gr noise originates from a distance of less than 40 micrometers from the surface (and periphery of the dot), since this is the minority carrier diffusion distance (the optical absorption depth is less than 10 micrometers).

Nevertheless, as the dot diameter increases, the 1/f noise has a much larger magnitude than simple dimensionality will permit. Thus, the generating origin of 1/f noise is small and localized, and yet appears to influence a much larger volume of the material. This result strongly supports the macroscopic point of view, as suggested by Teitler and Osborne[12, 13] and Handel[14] in the hydrodynamic analogy. From this point of view the non-linear dissipation in energy in recombination near the surface leads to fluctuations in the macroscopic current flow, analagous to turbulent mechanisms in fluid flow.

SECTION 11

INITIAL APPLICATION OF TECHNIQUE

11.1 GENERAL APPROACH

The above model has considerable significance for control of 1/f noise in devices such as (Hg,Cd)Te detectors. It suggests that, as initially discussed in Section 5, in order to reduce 1/f noise one should first determine the origin of the controlling nonlinearity mechanism which initiates macroscopic current fluctuations, then concentrate either on reducing the nonlinearity or the mechanism itself. Our observations have pinpointed minority carrier recombination mechanisms near the surface as the initiator in (Hg,Cd)Te detectors.

Methods for control of 1/f noise due to this phenomenon can be developed in a number of ways. One begins by noting that minority carrier recombination near the surface is determined by two independent parameters: (1) The recombination probability--usually due to recombination centers existing near or at the surface. (2) The arrival rate of minority carriers in this region. Recombination centers on the surface can be controlled by fabrication and processing procedures. Minority carrier motion can be strongly determined by surface space charge regions (as discussed in Section 5, they are related to depletion, inversion, and accumulation regions, with the latter preferred).

11.2 DIRECTIONS FROM PARALLEL PLATE RESULTS

Figure 11.1 shows the frequency spectrum of the noise obtained from parallel plates on two slabs. The results shown in this figure are typical of the data obtained on many elements of many slabs. The inverse frequency dependence is found to be linear, and all such data are stable and reliable.

It is notable that the 1/f corner frequency is considerably lower than usually observed on detectors. Therefore, one is immediately led to investigate detector processing conditions which could contribute to additional 1/f noise. The result of initial experiments of this nature is illustrated in Figure 11.2 which shows the application of the technique to determination of the effect of surface processing procedures on 1/f noise. The upper curve is the parallel-plate spectrum for surfaces prepared by process A. When the surface condition was charged to indicate detector processing procedures, the spectrum became that of the upper curve. Note the large increase in 1/f noise and carrier frequency.

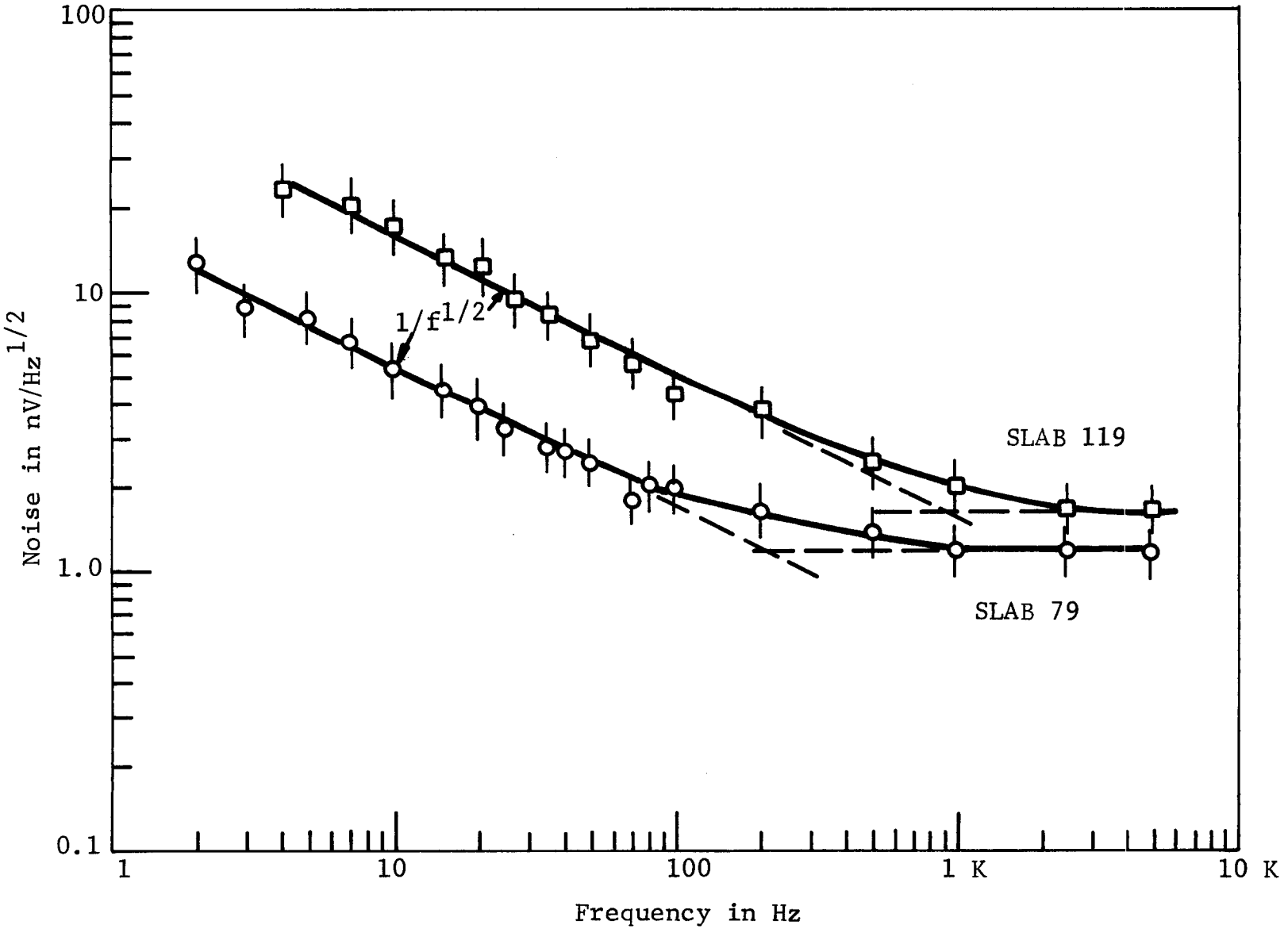

Figure 11.1 TYPICAL NOISE FREQUENCY SPECTRA ON SLABS (PARALLEL PLATES)

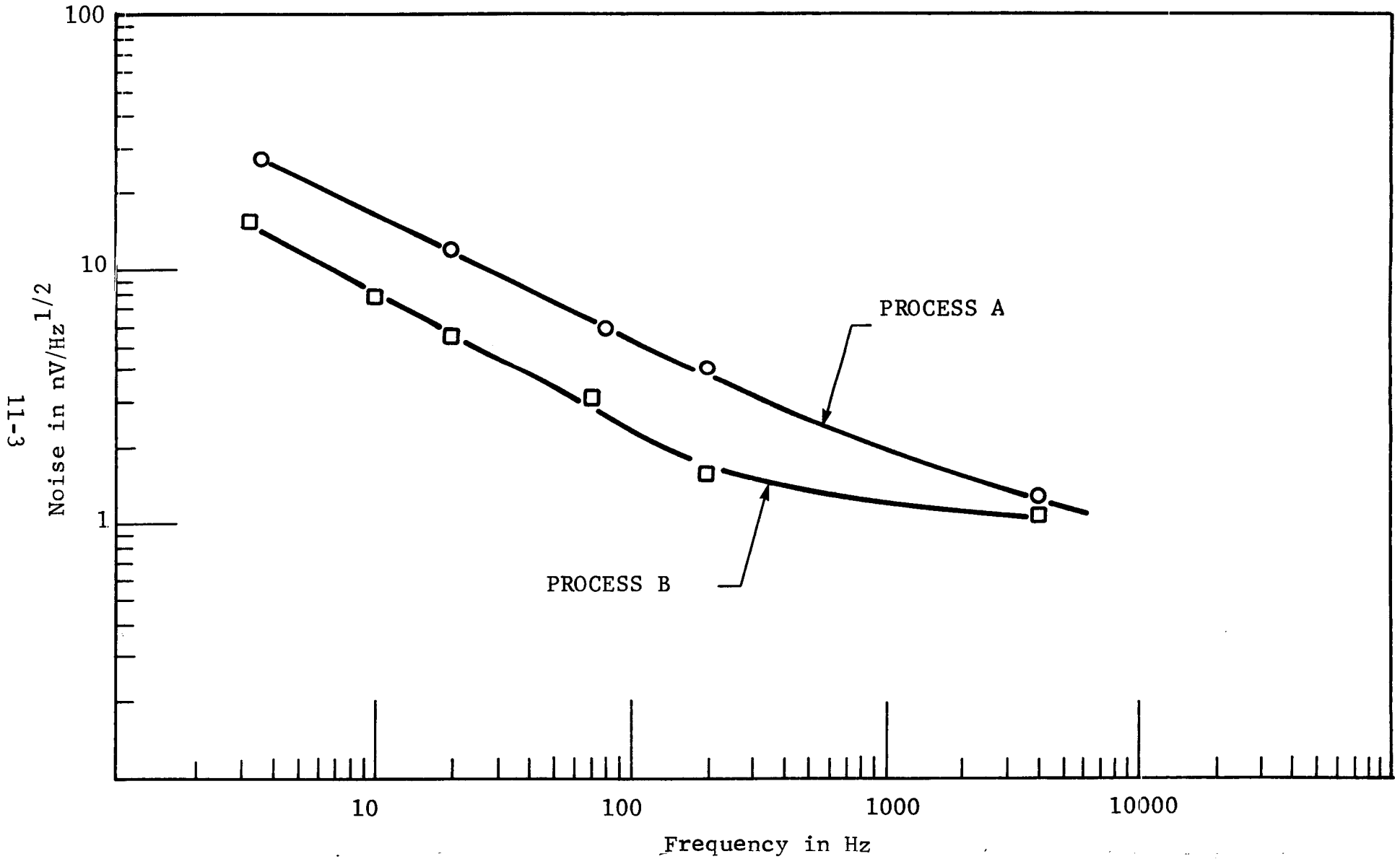

Figure 11.2 EFFECT OF SURFACE PROCESSING ON 1/f NOISE (PARALLEL PLATES)

SECTION 12

FIELD DEPENDENT EFFECTS — 1/f NOISE AND SWEEPOUT IN DETECTORS

Recent developments at the Radiation Center have indicated the significance of high field effects for several modes of detector operation. As the voltage across a high performance detector is increased, the signal level increases linearly at first with voltage, then less rapidly, and eventually saturates. It is known that the signal saturation is caused by the sweepout of minority carriers which, at higher field levels, reach the contacts before recombining in the active area of the detector.

Sweepout behavior is interesting not only for the applicability to high performance operation, but also because it relates directly to noise mechanisms. At low fields recombination occurs in the detector and at high fields at the contacts. Thus g-r noise changes character entirely; in fact, it has been proposed that g-r noise no longer exists in sweepout, but is replaced by the shot noise due to fluctuations in carriers arriving at the contacts. The spectral behavior of noise in sweepout has been recently considered by Williams[15], and the theory was originally derived by Hill and van Vliet[16]. Some results have been reported by Emmons and Ashley[17].

In view of our interest in the relationship between 1/f and g-r noise, it appeared desirable to initiate some investigations into field dependent 1/f noise in high performance detectors.

The high field dependence of 1/f noise was examined by looking at several detectors with fraction-of-BLIP detectivities. A spectrum of the low frequency noise was taken and the characteristic 1/f dependence found. The 20 Hz noise was taken at different bias levels in order to determine the field dependence of the 1/f noise (at 20 Hz the noise is all 1/f, the g-r component is negligible).

Figure 12.1 shows a typical field-dependence. Note the linear behavior at low bias levels and the marked departure from linearity beginning around 1 mA. At 4 mA the 1/f noise actually begins

CLASSIFICATION

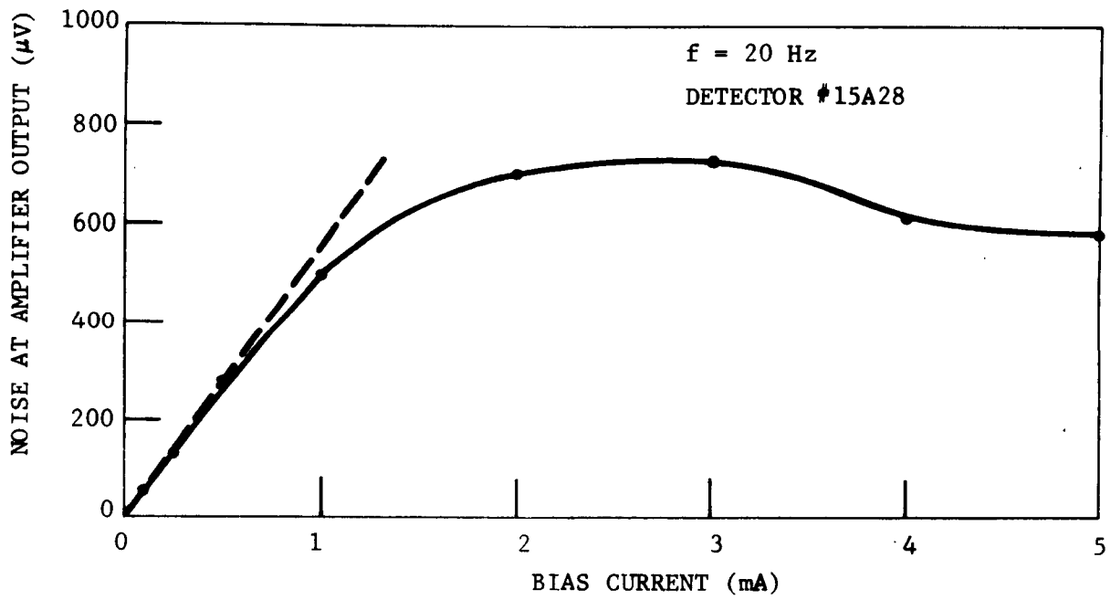

Figure 12.1 1/f NOISE VS BIAS ON DETECTOR

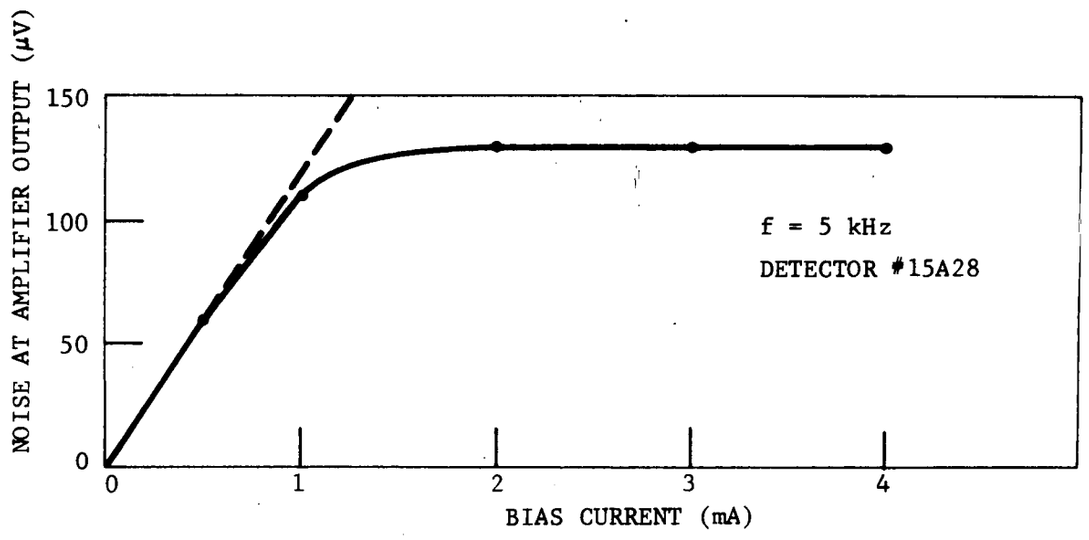

Figure 12.2 g-r NOISE VS BIAS ON DETECTOR

PCT

DO NOT TYPE BELOW THIS LINE

TYPE
PROOF
CORR
CKD

CLASS

decreasing as the field is further increased. Figure 12.3 shows the 5 kHz noise dependence on field. At this frequency the 1/f noise is negligible and the noise is g-r dominated. The flattening of the field dependence of high frequency noise is understood as an indication of minority carrier sweepout. Thus the field dependence of the 1/f noise (measured at 20 Hz) may be also related to sweepout via the correlation with g-r noise.

Unfortunately the heating due to power dissipated usually prohibited the gathering of reliable data at higher bias levels. However it was possible to obtain results for a high resistance detector which probably were not appreciably affected by heating.

The noise data for this detector are shown in Figure 12.4. Note that for low fields the 20 Hz noise is linearly dependent on the E field, but at 0.75 mA, the typical saturation due to sweepout appears. At 3 mA, however, the noise begins once again to increase linearly. An obvious interpretation is that there are two sources of 1/f noise, one of which rolls off at high fields and the other continues increasing linearly.

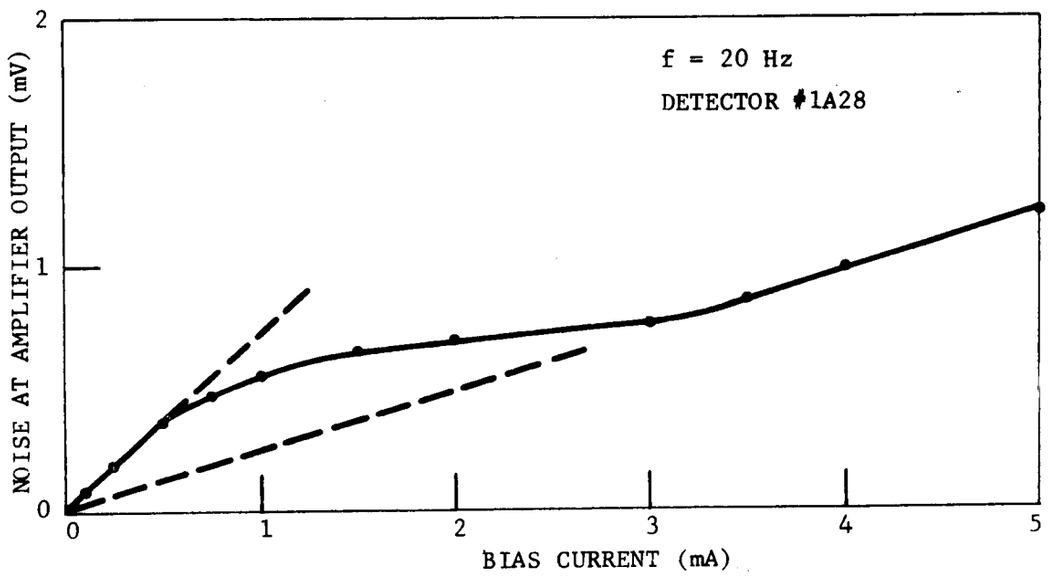

Figure 12.3 1/f NOISE VS BIAS ON DETECTOR

SOLID

CLASSIFICATION (If Any)

REFERENCES

1. J.J. Schlickman, "Mercury Cadmium Telluride Intrinsic Photodetectors," Proc. of the Electro-Optical Design Conference, p. 289, New York City, Sept. 1969.

2. D. Long and J.L. Schmit, "Mercury Cadmium Telluride and Closely Related Alloys, "Semiconductors and Semimetals, 5 p. 175, (Academic Press, New Yrok, 1970).

3. P.W. Kruse, L.D. McGlauchlin and R.B. McQuistan, Elements of Infrared Technology, p.252 (Wiley, New York, 1963).

4. H. Halpert and T. Koehler, "Study for Advanced Development of 15-Micron (Hg,Cd)Te Detectors," Final Report for Contract No. NAS 1-8996, April, 1970.

5. Van der Ziel, "Fluctuation Phenomena in Semiconductors," London, Butterworth' Scientific Publications (1959).

6. A. Van der Ziel, "Noise in Solid State Devices and Lasers," Proc. IEEE 58, 1178 (1970).

7. L.C. White, Proc. IRIS 13, 2315 (1969).

8. F.N. Hooge, "1/f Noise is No Surface Effect," Phys. Lett. 29A, 129 (1969).

9. W. Scott and R.J. Hager, "Anomalous Electrical Properties of p-type $Hg_{1-x}Cd_xTe$," J. App. Phys. 43, 803 (1971).

10. W. Scott, "Electron Mobility in $Hg_{1-x}Cd_xTe$," Jour. App. Phys. 43, 1055 (1972).

11. H. Fu and C. Sah, "Theory and Experiments on Surface 1/f Noise," IEEE Trans. Elec. Dve. ID-19, 273 (1972).

12. S. Teitler and M.F.M. Osborne, "Similarity Arguments and an Inverse-Frequency Noise Spectrum for Electrical Conductors," Phys. Rev. Letters 28, 912 (1971).

13. S. Teitler and M.F.M. Osborne, "Phenomenological Approach to Low Frequency Electrical Noise," Jour. App. Phys. 41, 3274 (1970).

PCF

CLASSIFICATION (If Any)

DO NOT TYPE BELOW THIS LINE